



# Benzotriazole-oxadiazole hybrid Compounds: Synthesis, anticancer Activity, molecular docking and ADME profiling studies



Arif Mermer<sup>a,\*</sup>, Muhammet Volkan Bulbul<sup>b,c</sup>, Semiha Mervener Kalender<sup>b</sup>, Ilknur Keskin<sup>b</sup>, Burak Tuzun<sup>d</sup>, Ozan Emre Eyupoglu<sup>e</sup>

<sup>a</sup> University of Health Sciences Turkey, Experimental Medicine Research and Application Center, Uskudar, 34662, Istanbul, Turkey

<sup>b</sup> Department of Histology and Embryology, School of Medicine, Istanbul Medipol University, Beykoz, 34810, Istanbul, Turkey

<sup>c</sup> Department of Histology and Embryology, Faculty of Medicine, Nisantasi University, Sariyer, 34398, Istanbul, Turkey

<sup>d</sup> Plant and Animal Production Department, Technical Sciences Vocational School of Sivas, Sivas Cumhuriyet University, Sivas, Turkey

<sup>e</sup> Department of Biochemistry, School of Pharmacy, Istanbul Medipol University, Beykoz, 34810, Istanbul, Turkey

## ARTICLE INFO

### Article history:

Received 25 November 2021

Revised 22 April 2022

Accepted 25 April 2022

Available online 29 April 2022

### Keywords:

Benzotriazole

Oxadiazole

Anticancer Activity

Molecular Docking

ADME

## ABSTRACT

Herein the designed novel benzotriazole-oxadiazole hybrid compounds were synthesized using both conventional method and ultrasound sonication (US) as an environmentally friendly method. It was observed that the US method provided an increase in reaction yields by reducing the reaction time approximately 3-fold. The synthesized compounds were investigated against PANC-1 cell line. All obtained compounds were characterized by FT-IR, <sup>1</sup>H NMR, <sup>13</sup>C NMR and MS spectroscopic techniques. The compounds **4b** and **4d** exhibited very promising anticancer activity results with IC<sub>50</sub> values of 117.5 ± 0.084 μM and 87.82 ± 4.319 μM, respectively. Further, molecular docking studies to suggest how the synthesized compounds interact with the kinase domain of human DDR1 in complex of pancreatic Cancer proteins (PDB ID: 6HP9), and the crystal structure of PDEd of pancreatic Cancer proteins (PDB ID: 5E80). It was concluded from the docking studies that the compound **4d** demonstrated the highest binding score values for active site of both proteins. Afterwards, ADME calculations were performed to examine the drug properties of benzotriazole-oxadiazole hybrid compounds.

© 2022 Elsevier B.V. All rights reserved.

## 1. Introduction

Cancer is potent to attack or expand to any parts of the body, and it continues as a significant reason of death worldwide [1,2]. The World Health Organization (WHO) guessed that one in five men and one in six women worldwide get cancer during their lifetime, and one in eight men and one in eleven women defeated to this deadliest disease [3]. In 2018, there were 18.1 million new cancer cases, leading to 9.6 million deaths [4,5]. Pancreatic adenocarcinoma (PAC) is the seventh leading cause of cancer-related death in both sexes, causing more than 331,000 deaths per year globally [6]. PAC is associated with an extremely poor prognosis reaching a 5-year overall survival (OS) rate below 5% [7] and 1-year OS rate at 24% based on standard treatments [4]. Even for patients with respectable disease, the prognosis is very poor, reflecting an OS rate of only 17% [8]. The poor prognosis is mainly due to lack of early symptoms, rapid tumor progression and limited efficacy of available drugs in locoregional/metastatic disease

[9]. Even though the cause of PAC is still not well understood, certain risk factors have been associated with PAC, such as advancing age, family history, smoking and alcohol use, male sex, diabetes mellitus and obesity [10]. Along with anticancer agents have an increasing importance in the treatment of cancer, more than 100 drugs against different types of cancer have been approved by the FDA and put into use for this purpose [11]. However, the many of them have improved multidrug resistance along with fatal side effects as well as low specificity, creating a huge demand for the improving of novel anticancer drugs with different mechanisms of action [12,13].

Benzotriazole is a sophisticated core in the field of medicinal chemistry and its derivatives are used by many researchers for therapeutic conditions [14]. In recent years, a wide range of biologically active compounds has been designed by researchers in which benzotriazole is acting as a nucleus itself or modulating the activity of other biologically active pharmacophores (Fig. 1). Benzotriazole derivatives designed so far has demonstrated potential biological activities such as antibacterial (1), antituberculosis (2), antifungal (3), antiviral (4), anticancer (5), and anti-inflammatory (6), etc. [15].

\* Corresponding author.

E-mail address: [arif.mermer@sbu.edu.tr](mailto:arif.mermer@sbu.edu.tr) (A. Mermer).

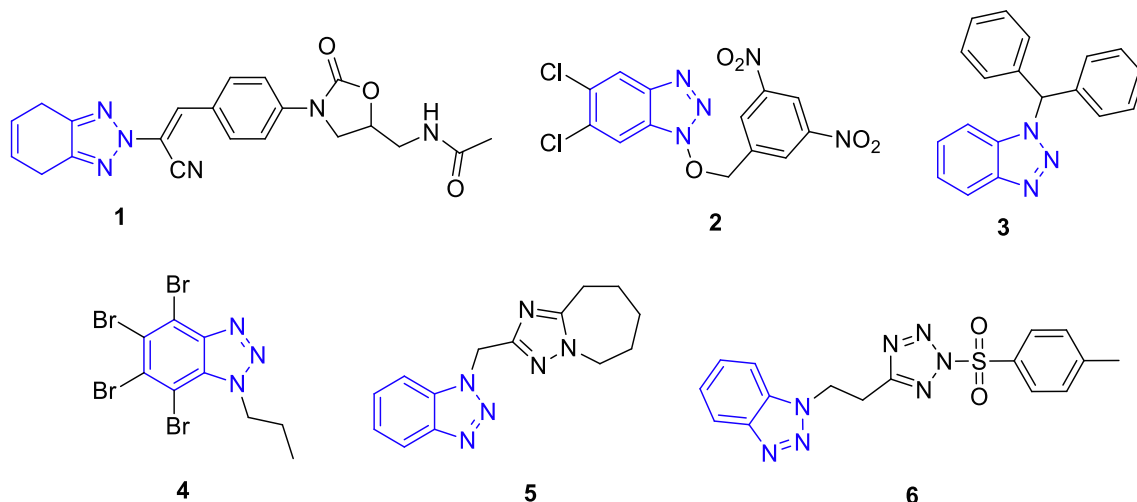


Fig. 1. Various biologically active benzotriazole derivatives.

Oxadiazole and its derivatives have recently attracted attention of various research groups due to their potency to be well bioisosteric replacement choices for several carbonyl including functional groups [16]. After the introduction of Furamizole and Nesapidil in the 1970 s, novel compounds raltegravir, ataluren and zibotentan, which contain oxadiazole ring in their structure, have been used in the treatment of cystic fibrosis or cancer in the following years [17]. The researchers have started to pay more attention to compounds containing the oxadiazole ring, and there have been numerous research articles and patent applications following this trend [18]. A wide range of pharmacological activities such as antibacterial (7), anti-TB (8), antifungal (9), anti-inflammatory (10), anticancer (11) have been exhibited by compounds including oxadiazole in their structure (Fig. 2) [19–23].

Molecular hybridization has the effect of enhancing affinity and activity of newly designed molecules, reducing side effects, and overcoming drug resistance by it based on the combination of two or more pharmacophore groups in a single structure [24,25]. Especially, lots of hybrid compounds such as Cefatrizine, Voreloxin, and Quarfloxin have been investigated under phase clinical trials or have already been used in clinics for the treatment of cancers, meaning this approach is a helpful process in the discovery of novel anticancer agents [26,27]. Apparently, hybridization of benzotriazole core with known anticancer pharmacophore, oxadiazole ring, may ensure novel anticancer candidates with low toxicity, high specificity, and great impact against drug-susceptible and drug-resistant cancers (Fig. 3).

Based on the previous findings and in continuation of our efforts in discovery of novel anticancer agents, novel benzotriazole-oxadiazole hybrid compounds were synthesized via conventional and ultrasound sonication methods as anticancer agents against PANC-1 cell line. Besides, theoretical methods which have shown a great development in the last 10 years with the developing technology were performed to understand how compounds interact with the active side of the proteins [28,29]. Pancreatic cancer proteins which are the structure of the kinase domain of human DDR1 in complex of pancreatic Cancer proteins (PDB ID: 6HP9) [30], and the crystal structure of PDEd of pancreatic Cancer proteins (PDB ID: 5E80) [31] were used in this study. Further, ADME profiles of the synthesized compounds were calculated.

## 2. Experimental section

### 2.1. Materials and instrumentation

All chemicals and solvents were purchased from Sigma Aldrich-Merck. Reactions were followed by thin-layer chromatography (TLC) on silica gel 60 F254 aluminum sheets. FTIR spectra were recorded using a ThermoFisher Scientific Nicolet IS50 FTIR spectrometer.  $^1\text{H}$  NMR and  $^{13}\text{C}$  NMR (APT) spectra were recorded on Bruker Avance II 400 MHz NMR spectrometer (chemical shift in ppm downfield from TMS as an internal reference). The mass spectra were achieved at a LC-MS TOF (1200/6210, Agilent) by electro-

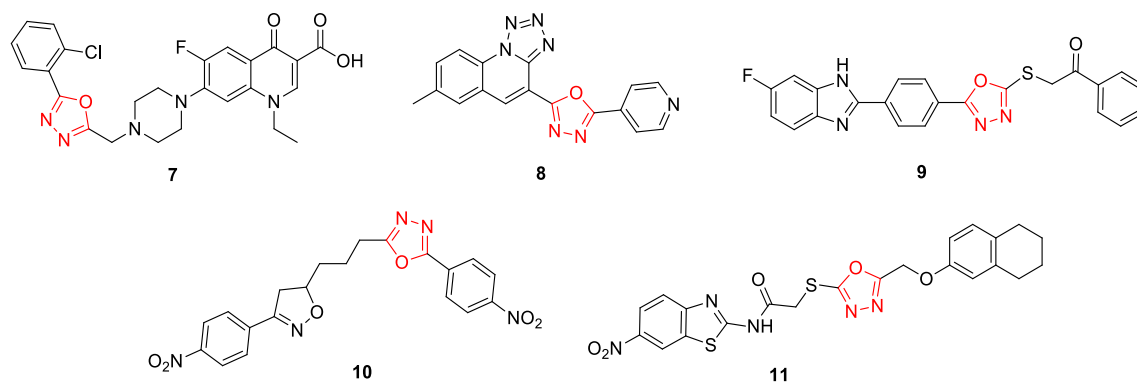


Fig. 2. Oxadiazole ring containing compounds with different biological activities.

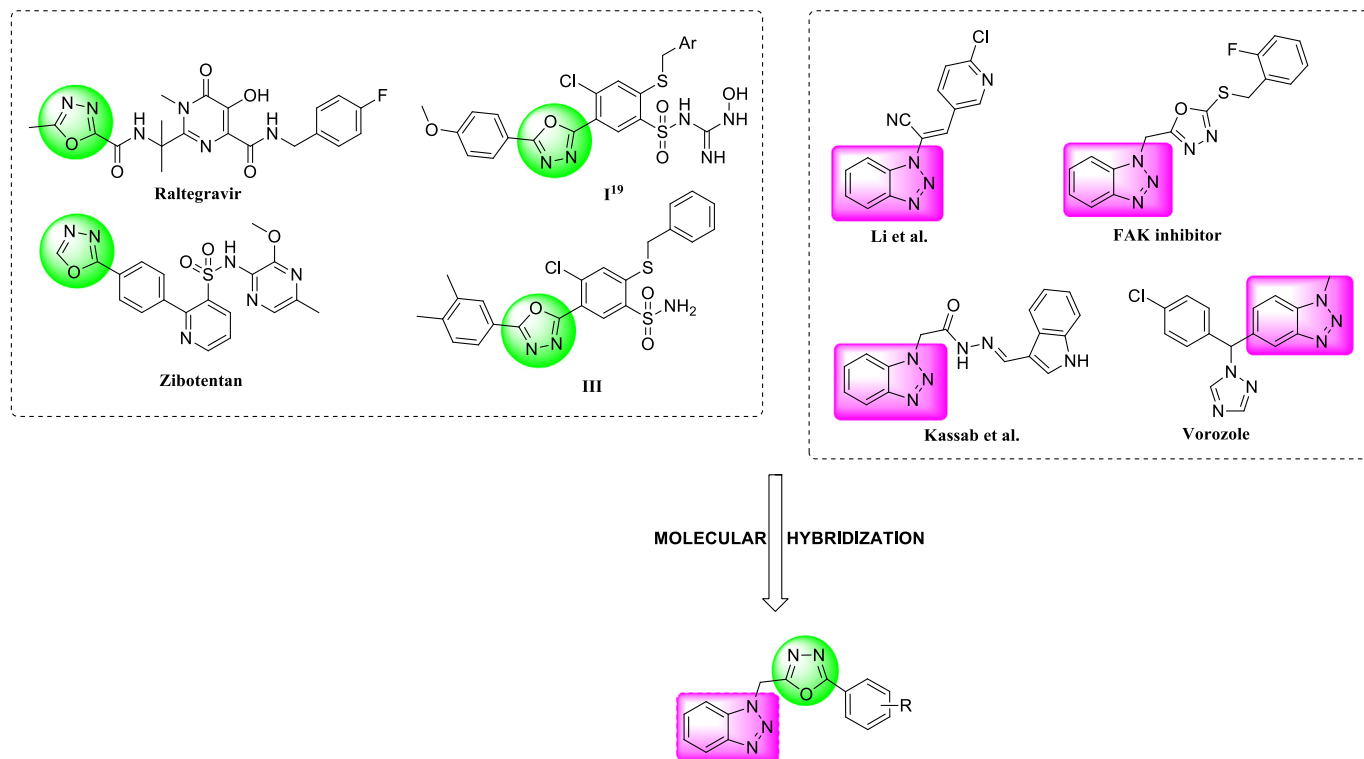


Fig. 3. Designing of target compounds via molecular hybridization.

spray ionization. The compounds **2** and **3** are known and synthesized by previously reported method [32,33].

## 2.2. General procedure for the synthesis of compounds 4a-4 m

**Method 1.** An equimolar mixture of compound **3** (10 mmol) and substituted aryl carboxylic acid (10 mmol) in phosphoryl chloride (10 mL) was refluxed for 10–16 h. Then the reaction mixture was cooled, poured into ice-cold water and neutralized with 20% NaHCO<sub>3</sub> solution. The formed solid was filtered, washed with water and recrystallized from ethanol to give the target compound.

**Method 2.** An equimolar mixture of compound **3** (10 mmol) and substituted aryl carboxylic acid (10 mmol) in phosphoryl chloride (10 mL) was sonicated at 35 °C, 40 Hz for 4–6 h in ultrasound bath. Then the reaction mixture was cooled, poured into ice-cold water and neutralized with 20% NaHCO<sub>3</sub> solution. The formed solid was filtered, washed with water and recrystallized from ethanol to give the target compound.

### 2.2.1. 1-[[5-(3,4-dimethylphenyl)-1,3,4-oxadiazol-2-yl]methyl]-1H-1,2,3-benzotriazole (4a)

Yield 72%, m.p. 236–238 °C. FT-IR ( $\nu_{\max}$ , cm<sup>-1</sup>): 3098.48 (ar-CH), 1508.11 (C = N). <sup>1</sup>H NMR (DMSO *d*<sub>6</sub>,  $\delta$ ppm): 2.26 (s, 6H, 2CH<sub>3</sub>), 6.45 (s, 2H, CH<sub>2</sub>), 7.31 (d, 1H, *J* = 8.0 Hz, arH), 7.43–7.47 (m, 1H, arH), 7.60–7.64 (m, 2H, arH), 7.70 (d, 1H, *J* = 8.0 Hz, arH), 7.94 (d, 1H, *J* = 8.0 Hz, arH), 8.10 (d, 1H, *J* = 8.0 Hz, arH). <sup>13</sup>C NMR (DMSO *d*<sub>6</sub>,  $\delta$ ppm): 19.66, 19.95, 42.64, arC: [114.09, 119.81, 120.81, 124.54, 124.89, 127.68, 128.46, 130.91, 133.43, 138.19, 141.83, 145.64], 161.64, 165.47. EI MS *m/z* (%): 274.92 (100), 305.86 ([M]<sup>+</sup>, 29).

### 2.2.2. 1-[[5-(3,4-dimethoxyphenyl)-1,3,4-oxadiazol-2-yl]methyl]-1H-1,2,3-benzotriazole (4b)

Yield 86%, m.p. 241–242 °C. FT-IR ( $\nu_{\max}$ , cm<sup>-1</sup>): 3066.07 (ar-CH), 1508.36 (C = N). <sup>1</sup>H NMR (DMSO *d*<sub>6</sub>,  $\delta$ ppm): 3.80 (s, 6H, 2OCH<sub>3</sub>), 6.45 (s, 2H, CH<sub>2</sub>), 7.11 (d, 1H, *J* = 8.0 Hz, arH), 7.40 (d, 1H,

*J* = 2.0 Hz, arH), 7.44–7.48 (m, 2H, arH), 7.60–7.64 (m, 1H, arH), 7.94 (d, 1H, *J* = 8.0 Hz, arH), 8.10 (d, 1H, *J* = 8.4 Hz, arH). <sup>13</sup>C NMR (DMSO *d*<sub>6</sub>,  $\delta$ ppm): 42.66, 56.08–56.16, arC: [109.56, 111.11, 112.46, 115.49, 119.81, 120.64, 124.88, 128.43, 133.43, 145.66, 149.52, 152.51], 161.45, 165.33. EI MS *m/z* (%): 274.92 (75), 338.06 ([M + 1]<sup>+</sup>, 100), 359.69 ([M + Na]<sup>+</sup>, 33).

### 2.2.3. 1-[[5-(4-trifluoromethylphenyl)-1,3,4-oxadiazol-2-yl]methyl]-1H-1,2,3-benzotriazole (4c)

Yield 65%, m.p. 238–240 °C. FT-IR ( $\nu_{\max}$ , cm<sup>-1</sup>): 3070.12 (ar-CH), 1479.48 (C = N). <sup>1</sup>H NMR (DMSO *d*<sub>6</sub>,  $\delta$ ppm): 6.51 (s, 2H, CH<sub>2</sub>), 7.86 (t, 3H, *J* = 10.0 Hz, arH), 8.04 (q, 3H, *J* = 4.0 Hz, arH), 8.13 (d, 2H, *J* = 8.0 Hz, arH). <sup>13</sup>C NMR (DMSO *d*<sub>6</sub>,  $\delta$ ppm): 42.63, arC: [111.12, 118.45, 119.81, 124.40, 124.89, 127.12, 127.96, 128.47, 128.84, 133.46, 134.11, 136.36, 145.43–145.63 (d, *J* = 10.0 Hz)], 162.61, 165.65. EI MS *m/z* (%): 346.05 ([M + 1]<sup>+</sup>, 42), 386.02 ([M + 1 + Na]<sup>+</sup>, 100).

### 2.2.4. 1-[[5-(3,4-dietoxiphenyl)-1,3,4-oxadiazol-2-yl]methyl]-1H-1,2,3-benzotriazole (4d)

Yield 79%, m.p. 243–245 °C. FT-IR ( $\nu_{\max}$ , cm<sup>-1</sup>): 3056.78 (ar-CH), 1508.11 (C = N). <sup>1</sup>H NMR (DMSO *d*<sub>6</sub>,  $\delta$ ppm): 1.30–1.34 (m, 6H, 2CH<sub>3</sub>), 4.03–4.09 (m, 4H, OCH<sub>2</sub>), 6.44 (s, 2H, CH<sub>2</sub>), 7.10 (d, 1H, *J* = 8.0 Hz, arH), 7.38 (d, 1H, *J* = 2.0 Hz, arH), 7.42 (d, 1H, *J* = 4.0 Hz, arH), 7.44 (q, 1H, *J* = 4.0 Hz, arH), 7.59–7.64 (m, 1H, arH), 8.08–8.11 (m, 1H, arH). <sup>13</sup>C NMR (DMSO *d*<sub>6</sub>,  $\delta$ ppm): 14.96–15.02, 42.65, 64.38–64.44, arC: [110.87, 111.11, 113.51, 115.33, 119.81, 120.61, 124.88, 128.43, 133.42, 145.65, 148.76, 151.93], 161.41, 165.31. EI MS *m/z* (%): 366.07 ([M + 1]<sup>+</sup>, 100), 388.05 ([M + Na]<sup>+</sup>, 45), 394.28 ([M + 1 + K]<sup>+</sup>, 99).

### 2.2.5. 1-[[5-(2-methylphenyl)-1,3,4-oxadiazol-2-yl]methyl]-1H-1,2,3-benzotriazole (4e)

Yield 84%, m.p. 230–231 °C. FT-IR ( $\nu_{\max}$ , cm<sup>-1</sup>): 3001.24 (ar-CH), 1540.93 (C = N). <sup>1</sup>H NMR (DMSO *d*<sub>6</sub>,  $\delta$ ppm): 2.33 (s, 3H, CH<sub>3</sub>), 6.49

(s, 2H, CH<sub>2</sub>), 7.47 (t, 1H, *J* = 6.0 Hz, arH), 7.56 (t, 1H, *J* = 6.0 Hz, arH), 7.60–7.64 (m, 1H, arH), 7.77 (d, 2H, *J* = 8.0 Hz, arH), 7.84 (d, 1H, *J* = 8.0 Hz, arH), 7.95 (d, 1H, *J* = 8.0 Hz, arH), 8.10 (d, 1H, *J* = 8.0 Hz, arH). <sup>13</sup>C NMR (DMSO *d*<sub>6</sub>, δppm): 21.65, 42.59, arC: [111.11, 119.49, 124.89, 125.97, 126.98, 128.45, 129.18, 130.96, 134.94, 136.24, 138.12, 145.54], 161.57, 165.54. EI MS *m/z* (%): 292.07 ([M + 1]<sup>+</sup>, 65), 309.99 ([M + H<sub>2</sub>O]<sup>+</sup>, 100).

#### 2.2.6. 1-[[5-(3,5-dimethoxyphenyl)-1,3,4-oxadiazol-2-yl]methyl]-1H-1,2,3-benzotriazole (4f)

Yield 87%, m.p. 244–246 °C. FT-IR (ν<sub>max</sub>, cm<sup>-1</sup>): 3084.30 (ar-CH), 1507.84 (C = N). <sup>1</sup>H NMR (DMSO *d*<sub>6</sub>, δppm): 3.76 (s, 6H, 2OCH<sub>3</sub>), 5.61 (s, 2H, CH<sub>2</sub>), 6.67 (t, 1H, *J* = 2.3 Hz, arH), 7.01 (d, 2H, *J* = 2.0 Hz, arH), 7.40 (t, 1H, *J* = 8.0 Hz, arH), 7.83 (d, 2H, *J* = 8.0 Hz, arH), 8.05 (d, 1H, *J* = 8.4 Hz, arH). <sup>13</sup>C NMR (DMSO *d*<sub>6</sub>, δppm): 49.09, 55.90, arC: [104.37, 105.72, 111.38, 119.51, 124.40, 125.29, 127.84, 133.09, 134.51, 145.53, 151.42, 152.50], 160.81, 165.61. EI MS *m/z* (%): 284.23 (56), 356.06 ([M + H<sub>2</sub>O]<sup>+</sup>, 79), 377.97 ([M + 1 + K]<sup>+</sup>, 100).

#### 2.2.7. 2-((1H-benzo[d][1,2,3]triazol-1-yl)methyl)-5-(naphthalen-2-yl)-1,3,4-oxadiazole (4g)

Yield 66%, m.p. 251–253 °C. FT-IR (ν<sub>max</sub>, cm<sup>-1</sup>): 3068.49 (ar-CH), 1519.37 (C = N). <sup>1</sup>H NMR (DMSO *d*<sub>6</sub>, δppm): 6.51 (s, 2H, CH<sub>2</sub>), 7.45 (t, 1H, *J* = 8.0 Hz, arH), 7.62 (q, 3H, *J* = 8.0 Hz, arH), 7.98 (t, 3H, *J* = 8.0 Hz, arH), 8.11 (d, 2H, *J* = 8.0 Hz, arH), 8.54 (s, 1H, arH). <sup>13</sup>C NMR (DMSO *d*<sub>6</sub>, δppm): 42.72, arC: [111.15, 119.83, 123.15, 124.91, 127.55, 127.82, 128.31, 128.48, 128.82, 129.38, 129.78, 145.67], 162.07, 165.53. EI MS *m/z* (%): 328.06 ([M + 1]<sup>+</sup>, 90), 345.98 (48), 349.97 (68), 367.96 ([M + K]<sup>+</sup>, 100).

#### 2.2.8. 1-[[5-(2-nitro-4-chlorophenyl)-1,3,4-oxadiazol-2-yl]methyl]-1H-1,2,3-benzotriazole (4h)

Yield 71%, m.p. 255–257 °C. FT-IR (ν<sub>max</sub>, cm<sup>-1</sup>): 3094.43 (ar-CH), 1537.07 (C = N). <sup>1</sup>H NMR (DMSO *d*<sub>6</sub>, δppm): 6.51 (s, 2H, CH<sub>2</sub>), 7.44 (t, 2H, *J* = 6.0 Hz, arH), 7.60 (t, 1H, *J* = 6.0 Hz, arH), 7.90 (d, 2H, *J* = 8.0 Hz, arH), 7.98 (s, 2H, arH), 8.08 (d, 1H, *J* = 8.0 Hz, arH). <sup>13</sup>C NMR (DMSO *d*<sub>6</sub>, δppm): 42.38, arC: [111.01, 115.56, 119.79, 124.89, 125.34, 128.48, 132.97, 133.40, 133.98, 138.29, 145.60], 161.16, 163.01. EI MS *m/z* (%): 357.04 ([M + 1]<sup>+</sup>, 100), 375.03 ([M + H<sub>2</sub>O]<sup>+</sup>, 65), 397.01 (83).

#### 2.2.9. 2-((1H-benzo[d][1,2,3]triazol-1-yl)methyl)-5-(quinolin-3-yl)-1,3,4-oxadiazole (4i)

Yield 63%, m.p. 249–251 °C. FT-IR (ν<sub>max</sub>, cm<sup>-1</sup>): 3059.99 (ar-CH), 1494.64 (C = N). <sup>1</sup>H NMR (DMSO *d*<sub>6</sub>, δppm): 6.55 (s, 2H, CH<sub>2</sub>), 7.38–7.47 (m, 3H, arH), 7.56 (q, 2H, *J* = 8.0 Hz, arH), 7.63 (t, 1H, *J* = 8.0 Hz, arH), 7.75 (t, 2H, *J* = 6.0 Hz, arH), 7.88 (d, 1H, *J* = 8.0 Hz, arH). <sup>13</sup>C NMR (DMSO *d*<sub>6</sub>, δppm): 42.69, arC: [111.40, 119.51, 124.42, 124.93, 127.85, 128.50, 129.36, 129.81, 130.25, 134.09, 145.33, 147.91], 163.15, 165.54. EI MS *m/z* (%): 328.97 ([M]<sup>+</sup>, 39), 347.03 ([M + H<sub>2</sub>O]<sup>+</sup>, 100).

#### 2.2.10. 1-[[5-(3-methoxy-4-hydroxyphenyl)-1,3,4-oxadiazol-2-yl]methyl]-1H-1,2,3-benzotriazole (4j)

Yield 89%, m.p. 233–235 °C. FT-IR (ν<sub>max</sub>, cm<sup>-1</sup>): 3078.22 (ar-CH), 1506.73 (C = N). <sup>1</sup>H NMR (DMSO *d*<sub>6</sub>, δppm): 3.86 (s, 3H, OCH<sub>3</sub>), 6.40 (s, 2H, CH<sub>2</sub>), 7.07 (s, 1H, arH), 7.11 (d, 1H, *J* = 8.0 Hz, arH), 7.17 (s, 1H, arH), 7.34 (s, 2H, arH), 7.43 (d, 1H, *J* = 4.6 Hz, arH), 7.67 (s, 1H, arH), 9.63 (s, 1H, OH). <sup>13</sup>C NMR (DMSO *d*<sub>6</sub>, δppm): 45.15, 57.65, arC: [110.87, 111.11, 115.98, 119.62, 121.33, 124.16, 127.81, 134.28, 144.55, 150.20, 153.40], 160.09, 164.41. EI MS *m/z* (%): 258.26 (39), 324.00 ([M + 1]<sup>+</sup>, 100), 328.97 (53), 356.13 (73).

#### 2.2.11. 1-[[5-(4-hydroxyphenyl)-1,3,4-oxadiazol-2-yl]methyl]-1H-1,2,3-benzotriazole (4k)

Yield 81%, m.p. 226–228 °C. FT-IR (ν<sub>max</sub>, cm<sup>-1</sup>): 3186.48 (OH), 3044.72 (ar-CH), 1524.02 (C = N). <sup>1</sup>H NMR (DMSO *d*<sub>6</sub>, δppm): 5.37 (s, 1H, OH), 6.31 (s, 2H, CH<sub>2</sub>), 7.35 (s, 1H, arH), 7.43 (d, 2H, *J* = 8.0 Hz, arH), 7.53 (t, 1H, *J* = 8.0 Hz, arH), 7.63 (d, 2H, *J* = 8.0 Hz, arH), 7.77 (d, 2H, *J* = 8.0 Hz, arH). <sup>13</sup>C NMR (DMSO *d*<sub>6</sub>, δppm): 49.12, arC: [111.23, 118.33, 119.47, 120.69, 122.59, 123.16, 124.39, 127.88, 129.56, 134.09, 145.53, 159.58], 165.66, 169.08. EI MS *m/z* (%): 226.74 (48), 238.99 (100), 316.90 ([M + Na]<sup>+</sup>, 91).

#### 2.2.12. 4-(5-((1H-benzo[d][1,2,3]triazol-1-yl)methyl)-1,3,4-oxadiazol-2-yl)benzene sulfonamide (4l)

Yield 73%, m.p. 242–244 °C. FT-IR (ν<sub>max</sub>, cm<sup>-1</sup>): 3079.81 (ar-CH), 1527.34 (C = N). <sup>1</sup>H NMR (DMSO *d*<sub>6</sub>, δppm): 6.21 (s, 2H, CH<sub>2</sub>), 7.34 (s, 2H, NH<sub>2</sub>), 7.44 (d, 2H, *J* = 5.2 Hz, arH), 7.58 (d, 2H, *J* = 4.8 Hz, arH), 7.76 (d, 2H, *J* = 8.0 Hz, arH), 8.75 (d, 2H, *J* = 4.6 Hz, arH). <sup>13</sup>C NMR (DMSO *d*<sub>6</sub>, δppm): 45.46, arC: [116.73, 124.24, 126.13–126.16 (d, *J* = 3.0 Hz), 126.33, 129.67, 130.09, 133.92, 142.20, 143.03, 159.82], 162.33, 166.98. EI MS *m/z* (%): 303.90 (100), 325.67 (74), 357.87 ([M + 1]<sup>+</sup>, 82).

#### 2.2.13. 1-[[5-(4-ethylphenyl)-1,3,4-oxadiazol-2-yl]methyl]-1H-1,2,3-benzotriazole (4m)

Yield 85%, m.p. 228–230 °C. FT-IR (ν<sub>max</sub>, cm<sup>-1</sup>): 3055.76 (ar-CH), 1522.36 (C = N). <sup>1</sup>H NMR (DMSO *d*<sub>6</sub>, δppm): 1.16 (t, 2H, *J* = 8.0 Hz, CH<sub>3</sub>), 2.63 (q, 2H, *J* = 4.0 Hz, CH<sub>2</sub>), 5.61 (s, 2H, CH<sub>2</sub>), 7.30 (d, 2H, *J* = 8.0 Hz, arH), 7.40 (t, 1H, *J* = 8.0 Hz, arH), 7.56 (t, 1H, *J* = 8.0 Hz, arH), 7.78 (d, 2H, *J* = 8.0 Hz, arH), 7.84 (d, 1H, *J* = 8.0 Hz, arH), 8.04 (d, 1H, *J* = 8.0 Hz, arH). <sup>13</sup>C NMR (DMSO *d*<sub>6</sub>, δppm): 15.71, 28.49, 49.11, arC: [111.41, 119.50, 124.39, 127.82, 128.00, 128.28, 130.05, 134.10, 145.54, 148.54], 158.75, 165.63. EI MS *m/z* (%): 306.98 ([M + 1]<sup>+</sup>, 78), 329.04 ([M + 1 + Na]<sup>+</sup>, 100).

### 2.3. Molecular docking studies

Molecular docking calculations were performed to observe the interaction between synthesized compounds and selected active site of proteins. The program developed by Maestro Molecular modeling platform (version 12.8) by Schrödinger [34] was used for molecular docking calculations. Calculations were made up of several steps, and each of them was done differently. In the first step, the protein preparation module [35] was used in the preparation of proteins. In this module, obtained compounds were prepared following the determination of the active sites of the proteins. Firstly, the compounds were optimized in the gaussian software program, then the LigPrep module [36] was prepared for calculations using optimized structures. The Glide ligand docking module [37] was used to examine the interactions between the molecules and the cancer protein after preparation. Calculations were made using the OPLS3e method in all calculations. Finally, ADME analysis (absorption, distribution, metabolism, and excretion) will be performed to examine the drug potential of the studied molecules. The Qik-prop module [38] of the Schrödinger software was used to predict the effects and reactions of molecules in human metabolism.

### 2.4. In vitro anticancer activity

#### 2.4.1. Cell culture

The PANC-1 (human pancreatic cancer) cell line was obtained from ATCC with the code CRL-1469. DMEM (Dulbecco's Modified Eagle's Medium) medium supplemented with 10% FBS (Fetal Bovine Serum) and 1% antibiotic-antimycotic solution was used for subculturing and all tests. During all experimental stages, cells



were incubated at 37 °C in a humid atmosphere of 5% CO<sub>2</sub> in 95% air. For trypsinization and counting of cells, the medium of the cells cultured in T75 flasks was aspirated. Cells were washed with sterile PBS. 750 µl of Trypsin/EDTA was added. After 2–3 min incubation, cells would be removed. After centrifugation at 1000 rpm for 3 min, the supernatant was removed. The pellet was mixed with 5 mL medium. The trypan blue exclusion test was used to calculate the number of viable cells. Cells were counted using a hemocytometer.

#### 2.4.2. In Vitro Cell viability assay

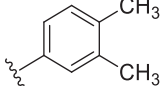
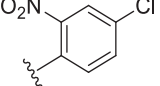
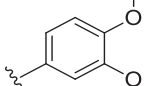
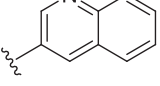
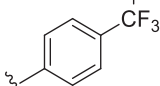
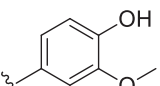
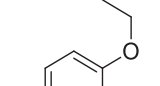
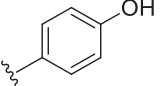
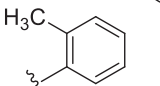
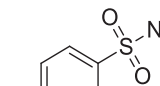
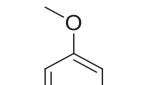
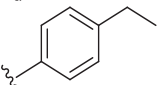
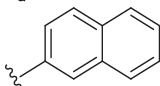
Colorimetric MTT ((3-(4,5-Dimethylthiazol-2-yl)-2,5-Diphenyl tetrazolium bromide) method was used to investigate the antiproliferative effect of synthesized compounds on PANC-1 cells. Cells were placed in 96-well plates with 2x10<sup>4</sup> cells in each well. They were cultivated as cells. To be confluent, they were incubated in 96-well plates for 24 h. Following the confluency of 70–80%, the medium on the wells was aspirated. The synthesized compounds were dissolved in DMSO to obtain high concentration stock solutions of each. Different concentrations of the compounds (10–500 µg/ml) were added to the cells with equal amounts of medium for incubation for 24 h. Eight replicates of all concentrations were made. Cells unexposed to any compound were used as negative control group, cells completely killed with Triton X as positive control group. At the end of the incubation periods, the medium on the cells and the compound mixtures were aspirated. MTT agent was added at a ratio of 1:20 (MTT agent: total medium) and incubated for 3 h (37 °C, 5% CO<sub>2</sub>). After incubation, MTT was aspirated. Solvent solution was added at a ratio of 1:1 (medium: DMSO) and incubated for 1 h in the dark in the orbital mixer. The absorbance of the resulting color change was measured with a spectrophotometer at 570 nm. Compound concentrations that caused a 50% reduction in proliferation of PANC-1 cells were considered as the IC<sub>50</sub> value. Nonlinear regression analyzes and concentration–response analyzes were performed using the GraphPad Prism 9.1 program [39].

### 3. Results and discussion

#### 3.1. Chemistry

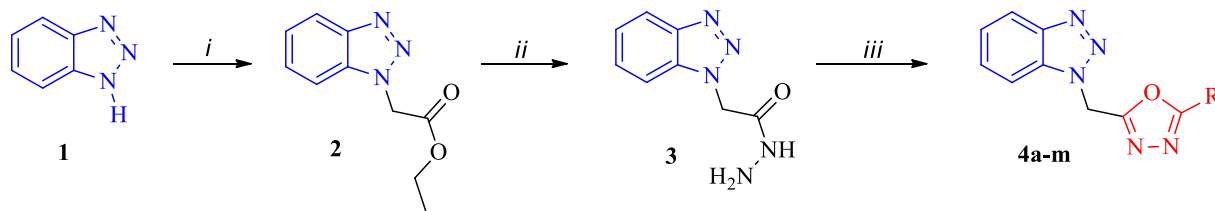
In present study, 13 benzotriazole-oxadiazole derivatives **4a–4m** were (Table 1) synthesized for the first time. The synthetic pathway of the novel compounds was given in Scheme 1. The compounds **2** and **3** were synthesized by previously described method. The hydrazide compound (**3**) was then treated with various aryl carboxylic acids in the presence of phosphoryl chloride, and oxadiazole ring was formed via an intramolecular cyclization reaction. The two methods, conventional and ultrasonication, were utilized to achieve the target compounds. Initially, considering the literature data [33,40], compound **4a** was selected as a model to determine the reaction time and yield. After the completion of the reaction, the synthesis of compound took 14 h with a yield of 63%. This result led us to the ultrasonication method, which is an environmentally friendly method to reduce the reaction time and increase the yield [41–43]. The same compound was chosen for optimization studies for ultrasound sonication, and by changing the conditions such as power (kHz), time (h) and temperature (°C), and yield (%), the optimization conditions for the highest reaction yield and the lowest reaction time were tried to be specified. In this reaction, US was found to be more effective than the conventional techniques, but the yields of the target compounds were modest in all the examples, even after several hours of sonication. We started by first applying low temperature, power, and reaction time to improve the appropriate reaction conditions. Trials were

**Table 1**  
The structure of synthesized compounds.

Compound	R	Compound	R
<b>4a</b>		<b>4h</b>	
<b>4b</b>		<b>4i</b>	
<b>4c</b>		<b>4j</b>	
<b>4d</b>		<b>4k</b>	
<b>4e</b>		<b>4l</b>	
<b>4f</b>		<b>4m</b>	
<b>4g</b>			

made by changing the power and temperature by keeping the reaction time constant, and because of these trials, the highest reaction yield was obtained at 35 °C and 40 kHz in 2 h (Entry 4). Based on this outcome, we wondered if increasing the reaction time influenced the reaction yield, and there was a slight increase in yield when the reaction time was increased to 3 h. When we increase the reaction time, it has been seen that the other conditions were 35 °C and 40 kHz as the optimum for the best reaction yield. Therefore, we again increased the reaction time from 3 h to 4 h, and the highest yield was obtained (Entry 8). However, it has been observed that when the temperature was increased at the same time (4 h), there is a decrease in the reaction yield and this situation also occurred when increasing the reaction time again (Entry 10). Thus, the best reaction condition under ultrasound sonication was obtained at 4 h, 35 °C and 40 kHz (Table 2). Although most of the compounds were synthesized at above reactions conditions, only compounds **4g** and **4i** were achieved 6 h with good-moderate yield.

The molecular structure of the obtained compounds was confirmed by spectroscopic methods containing FTIR, <sup>1</sup>H and <sup>13</sup>C NMR (APT), and mass spectrometry. In FTIR spectra, C = N bond vibrations in both benzotriazole and oxadiazole ring were



**Scheme 1.** Synthetic pathway of compounds 4a–4 m. *i*: THF, ethyl bromoacetate, rt. 24 h, *ii*: EtOH,  $\text{NH}_2\text{NH}_2 \cdot \text{H}_2\text{O}$ , reflux, 6 h, *iii*: Method 1: RCOOH,  $\text{POCl}_3$ , reflux, 10–16 h, Method 2: RCOOH,  $\text{POCl}_3$ , Ultrasound sonication, 4–6 h.

**Table 2**  
Optimization conditions for synthesizing compound **4a**<sup>[a]</sup>

Entry	Time (h)	Power (Hz)	Temp. (°C)	Yield (%)
1	2	30	30	52
2	2	30	35	54
3	2	35	40	58
4	2	40	35	60
5	3	30	35	58
6	3	30	35	62
7	3	35	40	66
<b>8</b>	<b>4</b>	<b>40</b>	<b>35</b>	<b>72</b>
9	4	40	40	70
10	5	40	35	68

<sup>[a]</sup>The reaction was performed by using **3** (10 mmol), 3,4-dimethylbenzoic acid (10 mmol) in the presence of phosphoryl chloride (10 mL) under US. The reaction was followed by TLC.

observed in the range of 1540.93–1494.64  $\text{cm}^{-1}$ . Further, the  $-\text{NH}$ ,  $-\text{NH}_2$  and  $\text{C}=\text{O}$  vibrations found in hydrazide compound (**3**) were not seen in oxadiazole derivatives. The  $^1\text{H}$  NMR spectra of all compounds demonstrated signals ranging from 6.67 ppm to 8.75 ppm indicating the presence of aromatic protons. Another proof for the formation of oxadiazole ring was that the  $-\text{CH}_2$  protons resonated at 4.62 ppm in compound **3** shifted to in the range of 5.61–6.51 ppm. Moreover, the disappearance of the carbonyl carbon in compound **3** and the detection of oxadiazole C-2 and oxadiazole C-5 carbons belonging to the oxadiazole ring also confirmed the structures spectroscopically. Similarly, all the synthesized benzotriazole-oxadiazole derivatives exhibited their respective  $m/z$  value peaks according to the molecular mass of the compounds.

### 3.2. Cytotoxicity in PANC-1 cancer cells

PANC-1 cell line is frequently used in the investigation of the cytotoxic effects of different chemotherapeutic agents such as capecitabine, cisplatin, fluorouracil, docetaxel, erlotinib, oxaliplatin, irinotecan, or active compounds such as curcumin, bacterial pigments such as pyocyanin,  $\text{Fe}_3\text{O}_4/\text{CdWO}_4$  nanoparticles, fungal metabolites such as (3S,6S)-3,6-dibenzylpiperazine-2,5-dione [44–48]. Therefore, in this study we investigated our synthesized compounds against PANC-1 cell line.

The cytotoxic effects of seven different doses (10–50–100–150–250–400–500  $\mu\text{g}/\text{ml}$ ) of the obtained compounds were investigated on the human pancreatic cancer cell line (PANC-1) using the MTT analysis method as described in the experimental section. Graph-Pad Prism 9.1 program was used for all statistical analyzes and determination of  $\text{IC}_{50}$  values.

As a result of MTT analysis, the  $\text{IC}_{50}$  values of all compounds on the PANC-1 cell line are shown in Table 3. Most of the synthesized compounds exhibited mild to moderate cytotoxicity results. The compound **4d** was found to be the most potent against PANC-1 cell line with an  $\text{IC}_{50}$  value of  $87.82 \pm 4.319 \mu\text{g}/\text{ml}$ . The compound **4b**

**Table 3**  
Antiproliferative activity results of the synthesized compounds against PANC-1 cell line

Compound	$\text{IC}_{50}$ ( $\mu\text{g}/\text{ml}$ )	SEM <sup>a</sup>
<b>4a</b>	340.5	$\pm 2.248$
<b>4b</b>	117.5	$\pm 0.084$
<b>4c</b>	125.8	$\pm 0.082$
<b>4d</b>	87.82	$\pm 4.319$
<b>4e</b>	204.4	$\pm 0.021$
<b>4f</b>	709.8	$\pm 0.431$
<b>4g</b>	252.9	$\pm 0.034$
<b>4h</b>	143.7	$\pm 0.025$
<b>4i</b>	124.9	$\pm 0.022$
<b>4j</b>	4650	nd <sup>*</sup>
<b>4k</b>	129.3	$\pm 1.742$
<b>4l</b>	714.9	$\pm 0.052$
<b>4m</b>	240.2	$\pm 0.032$

a: standard error mean, \*: not detected

containing 3,4-dimethoxyphenyl as a functional group linked to the oxadiazole C-5 position showed the second highest inhibition result with  $\text{IC}_{50}$  value of  $117.50 \pm 0.084 \mu\text{g}/\text{ml}$ , while the compound **4f** including 3,5-dimethoxyphenyl group displayed approximately 6-fold lower potency than compound **4b**. The compounds **4i**, **4c** and **4k** demonstrated similar activity results against the target cell line with  $\text{IC}_{50}$  values of  $124.90 \pm 0.022 \mu\text{g}/\text{ml}$ ,  $125.80 \pm 0.082 \mu\text{g}/\text{ml}$ , and  $129.30 \pm 1.742 \mu\text{g}/\text{ml}$ , respectively. Among the compounds, **4j** containing 3-methoxy-4-hydroxyphenyl as a functional group was found to have lowest activity result. **4j**'s  $\text{IC}_{50}$  değeri, kullanılan doz aralığının çok dışında ve istatistiksel olarak anlamsız bir değer ( $4650 \mu\text{g}/\text{ml}$ ) sergilediğinden dolayı gösterilmemiştir (Table 3).

The viability curves of the cytotoxic effects of different doses of the compounds on PANC-1 cells were displayed using the Graph-Pad Prism 9.1 program (Figs. 4–5). Considering the cell viability data are examined, the cytotoxic effects of compounds **4a**, **4c**, **4f**, **4h**, **4i**, and **4m** were directly related to concentration. Except for deviations at 150  $\mu\text{g}/\text{mL}$  dose in compound **4b** and 400  $\mu\text{g}/\text{mL}$  dose in compounds **4k** and **4g**, dose-related decrease in viability percentages was observed. In compound **4e**, on the other hand, the percentage of viability decreased depending on the dose without any deviation from the dose of 50  $\mu\text{g}/\text{mL}$ . It was observed that the compound **4d** decreased the vitality levels between 39.7% and 50.3% with very close increases and decreases. Similarly, although different viability levels ranging from 47.6% to 81.79% were detected for compound **4l**, the dose–response pattern was not exhibited. The compound **4j** had the highest lethality at a dose of 100  $\mu\text{g}/\text{ml}$  at 81.3% viability. When the effects of compounds on the percentage of viability on PANC-1 cells were examined in terms of the highest dose (500  $\mu\text{g}/\text{mL}$ ), the compounds **4a** (51%) and **4f** (58.8%) had the lowest cytotoxicity, compounds **4d** (47%), **4k** (46.8%), and **4l** (47.6%) low cytotoxicity, compounds **4b** (28.9%), **4g** (33.7%), **4i** (20.2%), and **4m** (28.4%) moderate cytotoxicity, compounds **4e** (6.5%) and **4h** (5%) exhibited high levels of cytotox-

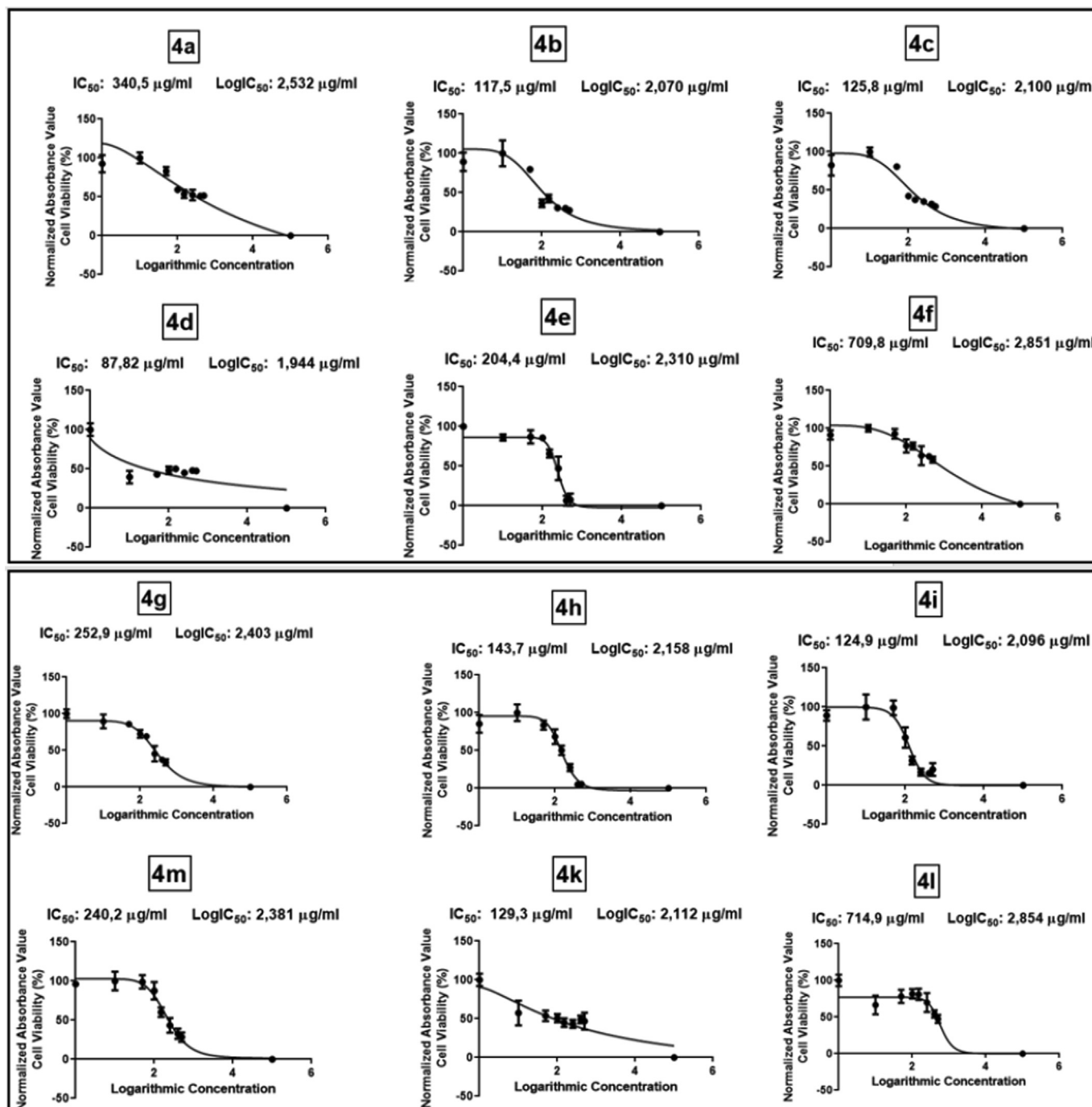


Fig. 4. Graphs of viability curves of 4a-4f compounds.

icity. Since the cells showed 100% viability at a dose of 500  $\mu\text{g/ml}$  for compound **4j**, it can be thought that this compound has almost no cytotoxic effect on PANC-1 cells (Table 4).

The dose-response relationship describes the magnitude of the organism's response rate with the exposure to a stimulant or stressor (usually a chemical) after a given exposure time [49]. Three general assumptions are considered when evaluating the dose-response relationship. 1) The chemical interacts with the molecule or receptor site to produce a response. 2) The degree of response is related to the concentration of the chemical at that receptor site. 3) The concentration of the chemical at the receptor site is related to the dose of the ingested chemical. For these reasons, there must

be a measurable effect on a true dose-response relationship proportional to the concentration of the chemical ingested [50].

Although compound **4d** showed the best potency against the PANC-1 cell line with the smallest  $IC_{50}$  value, the dose-dependent viability percentages were close to each other. These results suggest that the doses of this compound should be studied in a wider range in future studies. Therefore, it can be said that the anticancer potential of compound **4b** is higher than that of **4d**, because both it has the second strongest  $IC_{50}$  value and the viability curve exhibits a more suitable model for the dose-response relationship. No significant difference was observed between the 10  $\mu\text{g/ml}$  and 50  $\mu\text{g/ml}$  doses of compounds **4a** and **4b**, and the negative control (ns). While no significant difference was observed between the 50  $\mu\text{g/}$

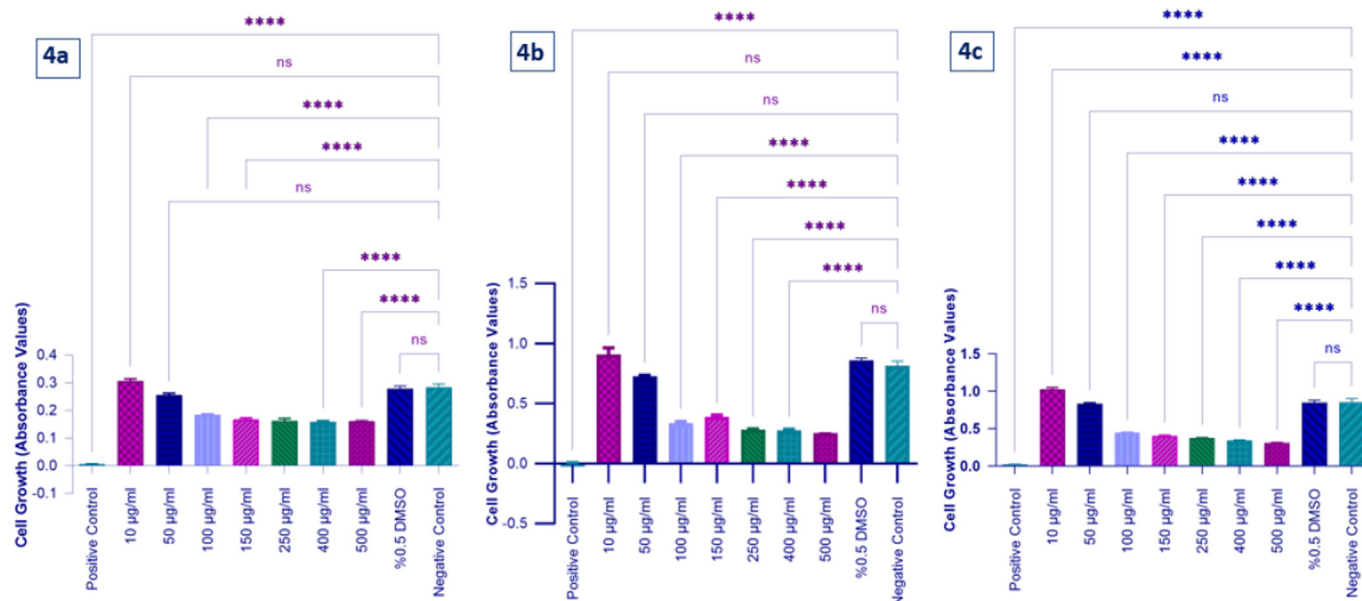


**Fig. 5.** Graphs of viability curves of 4 g-4 l Compounds. (Data for the compound **4j** is not shown.). (\*\*\*\*: Extremely significant, \*\*\*: Extremely significant, \*\*: Very significant, \*: Significant, ns: Not significant).

**Table 4**  
Percentage cell viability for compounds 4a-4 m at all doses

Cell viability (%) / SEM <sup>a</sup>							
Compound	10(µg/ml)	50(µg/ml)	100(µg/ml)	150(µg/ml)	250(µg/ml)	400(µg/ml)	500(µg/ml)
<b>4a</b>	100/ ±2.48	83.1/ ±1.9	59.7/ ±1.1	53.7/ ±1.8	52.3/ ±2.4	51/ ±1.3	51/ ±1.3
<b>4b</b>	100/ ±5.8	79.7/ ±1.1	36.6/ ±1.6	42.5/ ±1.7	30.7/ ±0.7	30.1/ ±0.9	27.6/ ±0.3
<b>4c</b>	100/ ±2	80.7/ ±1.1	42.4/ ±0.4	37.5/ ±0.5	35.2/ ±0.6	32.1/ ±0.5	28.9/ ±0.7
<b>4d</b>	39.7/ ±2.8	43.1/ ±1.2	48.4/ ±1.7	50.3/ ±1.1	45.1/ ±0.9	43/ ±1	47/ ±0.5
<b>4e</b>	86/ ±1.4	87.1/ ±2.9	85.6/ ±0.9	65.8/ ±1.7	47.2/ ±5.2	7.7/ ±2.2	6.5/ ±2.7
<b>4f</b>	100/ ±1.5	92.9/ ±2.2	76.9/ ±3	76.7/ ±1.5	64.1/ ±4.4	63.1/ ±1.3	58.8/ ±1.4
<b>4g</b>	89.5/ ±3.3	85.8/ ±1.1	72.5/ ±1.8	69.2/ ±1.2	45.4/ ±3.7	97.2/ ±1.1	33.7/ ±1.4
<b>4h</b>	100/ ±3.9	83.6/ ±2.1	68.4/ ±3.4	50.2/ ±2.1	27.4/ ±1.7	5/ ±0.3	5/ ±0.4
<b>4i</b>	100/ ±5.7	99/ ±3.3	61/ ±4.6	31.7/ ±1.8	16.7/ ±1.5	15.2/ ±0.6	20.2/ ±2.8
<b>4j</b>	89.1/ ±1.4	86.8/ ±1.7	81.3/ ±2.1	86.4/ ±2.4	85.3/ ±2	95.5/ ±3.4	100/ ±4.2
<b>4k</b>	57.3/ ±5.6	53.8/ ±2.3	50.6/ ±1.8	45/ ±1.9	43.3/ ±1.8	49.1/ ±1.7	46.8/ ±3.8
<b>4l</b>	66.6/ ±4.5	78.3/ ±3.2	81.79/ ±2.2	81.1/ ±2.8	69.9/ ±4.5	54.3/ ±1.7	47.6/ ±1.9
<b>4m</b>	100/ ±4.2	98.8/ ±3	87.6/ ±3.9	60.2/ ±2.1	43.4/ ±3.3	32.8/ ±2.3	28.4/ ±2

a: standard error mean

ml dose of compound **4c** and the negative control, the 10 µg/ml dose of compound **4c** demonstrated an extremely crucial proliferative effect without showing any cytotoxic effect (\*\*\*\*;  $p < 0.0001$ ). The compounds **4a**, **4b** and **4c** exhibited their cytotoxic effects from a dose of 100 µg/ml (\*\*\*\*;  $p < 0.0001$ ) (Fig. 6). When all doses of compound **4d** were compared with the negative control, it was noticed that it had an extremely significant cytotoxic effect (\*\*\*\*;  $p < 0.0001$ ). For compound **4e**, 10 µg/mL dose had a low level of significance but showed a cytotoxic effect when compared to the negative (\*;  $p < 0.01$ ). Further, the cytotoxic effect was observed at all doses from 100 µg/ml for compounds **4e** and **4f** (\*\*;  $p < 0.001$ , \*\*\*\*;  $p < 0.0001$ ) (Fig. 7). Unlike other compounds, the compound **4g** displayed a cytotoxic effect from the dose of 50 µg/mL (\*\*;  $p < 0.001$ , \*\*\*\*;  $p < 0.0001$ ). As with compound **4e**, compound **4h** exhibited important cytotoxic effect at a dose of 10 µg/mL (\*\*;  $p < 0.001$ ), while the cytotoxic effect of compound **4i** was observed from 100 µg/ml dose (\*\*\*\*;  $p < 0.0001$ ) (Fig. 8). While an extremely significant cytotoxic effect was observed at all doses for compound **4k** (\*\*\*\*;  $p < 0.0001$ ), no cytotoxic effects were seen at doses 50, 100 and 150 µg/mL doses for compound **4l** and 10, 50 and 100 µg/mL doses for compound **4m** (ns)

(Fig. 9). The highest dose (0.5%) of DMSO used as the solvent was determined as the solvent control group, and no cytotoxic effect was observed in the solvent control group in any of the experiments performed with the compounds (ns).

### 3.2.1. Molecular docking calculation

The activities of benzotriazole-oxadiazole hybrid compounds were compared using molecular docking method. With this method, the activities of compounds against pancreatic cancer proteins were examined, and there are some factors and effects that determine the activities of the compounds, the most important of which is the interaction between compounds and proteins. It was observed that as the chemical interactions between compounds and proteins increased, the activity of the molecules increased. These chemical interactions that occur are hydrogen bonds, polar and hydrophobic interactions,  $\pi$ - $\pi$  and halogen [51–54]. These interactions are given in Figs. 10–11. Many parameters obtained from these interactions between molecules and proteins are given in Table 5.

After the calculations, it is seen that in the interaction between compound **4d** with pancreatic Cancer proteins (6HP9), a hydrogen



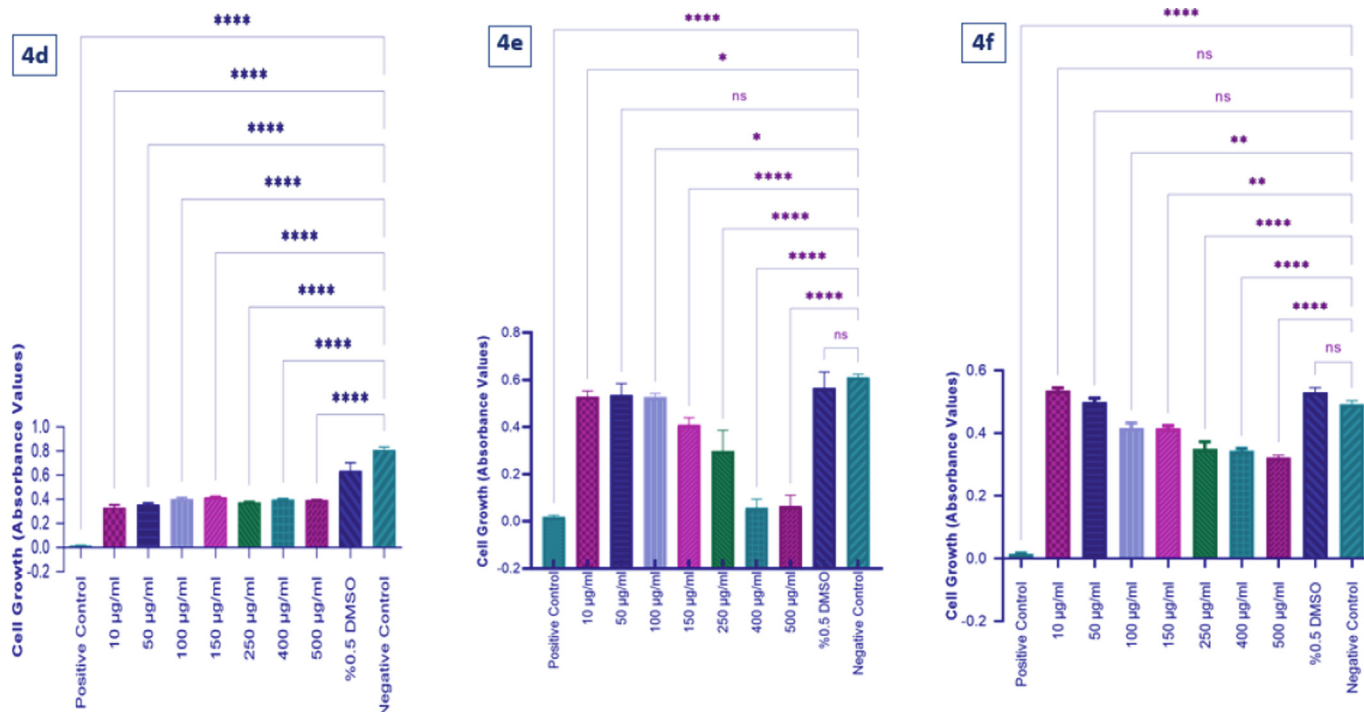


Fig. 6. Graph showing the differences in the doses of compounds 4a-4c on cell viability. (\*\*\*\*: Extremely significant, \*\*\*: Extremely significant, \*\*: Very significant, \*: Significant, ns: Not significant).

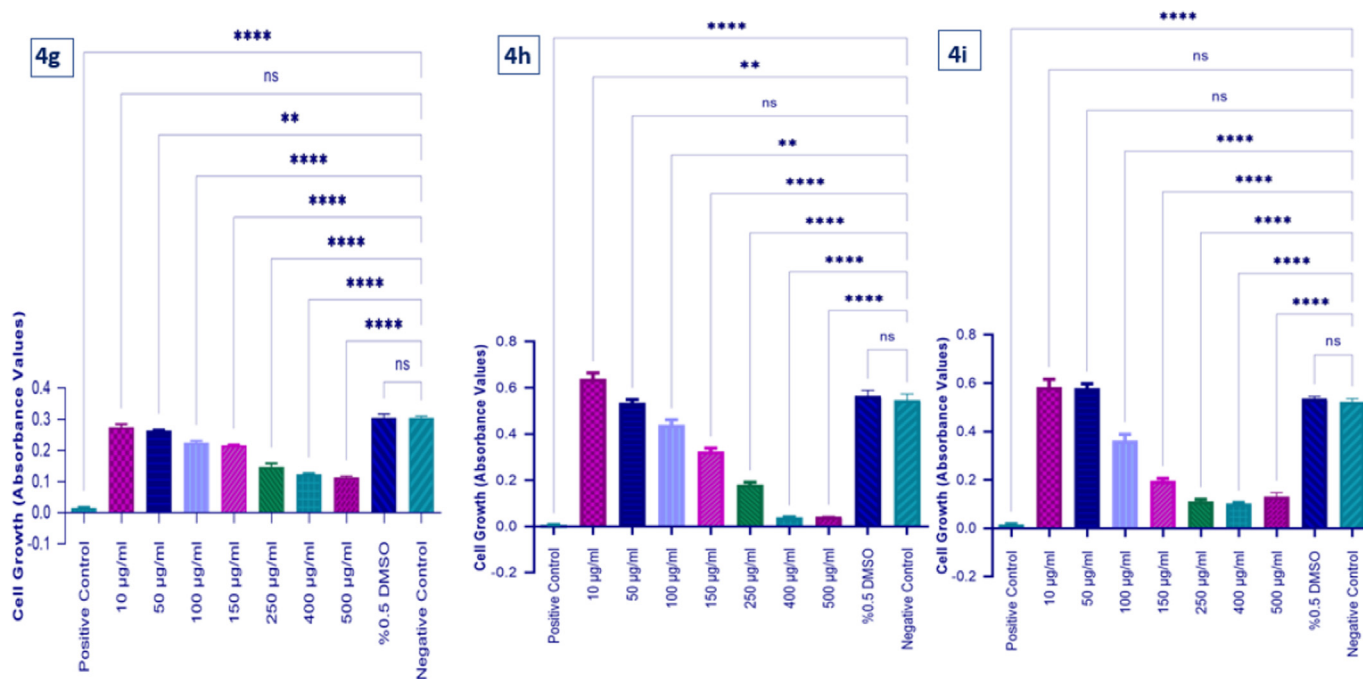


Fig. 7. Graph showing the differences in the doses of compounds 4d-4f on cell viability. (\*\*\*\*: Extremely significant, \*\*\*: Extremely significant, \*\*: Very significant, \*: Significant, ns: Not significant).

bond interaction occurs between the two nitrogen atoms in the benzotriazole ring, ARG 61 and GLN 78 proteins. Apart from this interaction, it makes polar and hydrophobic interactions with the proteins around the compound. In the interaction between compound 4d with pancreatic cancer proteins (5E80), nitrogen atoms in the oxadiazole ring in the center of the compound interact with the GLU 672 protein through hydrogen bonding. however, it

appears that the nitrogen atoms in the oxadiazole ring at the center of the compound interact with the PHE 785 protein. It was observed that as these interactions increased, the activities of the compounds increased.

The most important effect that determines the activity of compound 4d, which has the highest activity among compounds, is the occurred chemical interactions. Since the nitrogen atoms in the



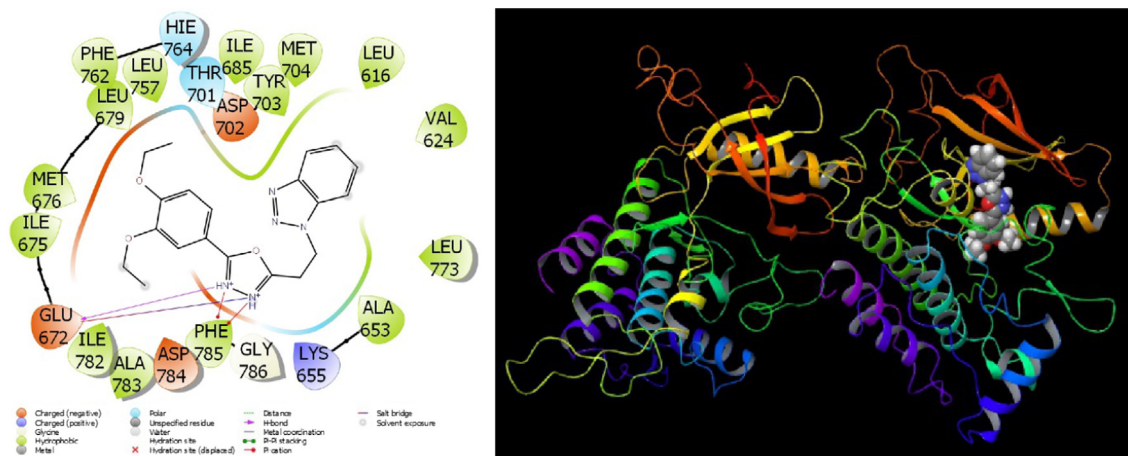


Fig. 10. Presentation interactions of molecule 4d with pancreatic Cancer proteins (6HP9).

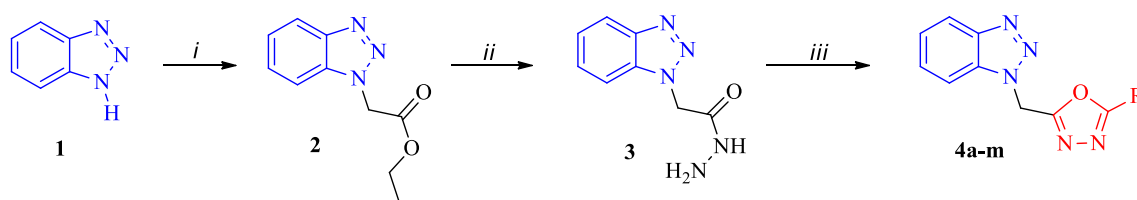


Fig. 11. Presentation interactions of molecule 4d with pancreatic Cancer proteins (5E80).

Table 5  
Numerical values of the docking parameters of compounds against enzymes

6HP9	4a	4b	4c	4d	4e	4f	4 g	4 h	4i	4j	4 k	4 l	4 m
Docking Score	-8.29	-8.35	-8.40	-8.71	-7.43	-8.18	-8.50	-6.38	-7.52	-8.08	-8.55	-7.09	-7.91
Glide ligand efficiency	-0.35	-0.32	-0.32	-0.28	-0.32	-0.34	-0.33	-0.25	-0.29	-0.32	-0.37	-0.27	-0.33
Glide hbond	-0.26	-0.20	-0.24	-0.19	-0.24	-0.38	-0.20	-0.06	0.00	-0.28	-0.21	-0.55	-0.20
Glide evdw	-37.71	-40.26	-35.48	-37.69	-35.96	-41.72	-38.91	-40.96	-39.81	-39.25	-31.97	-38.18	-35.84
Glide ecoul	-10.20	-10.98	-10.92	-9.05	-9.82	-8.36	-9.05	-2.54	-2.36	-10.83	-14.71	-7.98	-10.66
Glide emodel	-76.38	-80.36	-75.84	-67.10	-70.02	-84.15	-77.12	-60.10	-61.10	-78.93	-74.12	-64.59	-73.77
Glide energy	-47.91	-51.24	-46.40	-46.74	-45.78	-50.08	-47.96	-43.50	-42.17	-50.08	-46.68	-46.16	-46.50
Glide einternal	2.53	3.77	2.02	5.54	4.47	3.35	1.47	2.31	1.89	2.80	1.14	1.83	3.94
Glide posenum	208	256	314	126	4	350	240	205	349	230	296	124	175
<b>5E80</b>	<b>4a</b>	<b>4b</b>	<b>4c</b>	<b>4d</b>	<b>4e</b>	<b>4f</b>	<b>4 g</b>	<b>4 h</b>	<b>4i</b>	<b>4j</b>	<b>4 k</b>	<b>4 l</b>	<b>4 m</b>
Docking Score	-9.24	-8.75	-8.62	-9.52	-8.81	-8.82	-9.08	-8.58	-8.73	-9.01	-9.50	-8.14	-8.58
Glide ligand efficiency	-0.38	-0.34	-0.33	-0.30	-0.38	-0.34	-0.35	-0.33	-0.34	-0.36	-0.42	-0.31	-0.36
Glide hbond	0.00	0.00	0.00	0.00	0.00	0.00	0.00	0.00	0.00	0.00	-0.32	0.00	0.00
Glide evdw	-44.67	-42.24	-36.10	-46.95	-41.67	-46.76	-47.28	-45.77	-48.39	-46.11	-42.18	-45.47	-41.77
Glide ecoul	-3.05	-8.27	-5.29	-2.45	-3.83	-2.46	-1.93	-1.51	-1.99	-4.76	-8.54	-1.05	-3.64
Glide emodel	-71.55	-72.85	-62.27	-70.83	-68.72	-75.14	-72.26	-69.83	-72.96	-75.67	-79.30	-67.41	-67.64
Glide energy	-47.72	-50.50	-41.38	-49.40	-45.50	-49.22	-49.21	-47.28	-50.38	-50.86	-50.72	-46.53	-45.42
Glide einternal	3.10	7.22	1.75	10.15	2.14	1.10	4.99	2.35	4.66	4.72	2.00	0.94	2.59
Glide posenum	268	70	353	255	81	270	39	247	198	36	325	168	86

[59] (three of Jorgensen's rule). The numerical value of these two parameters is expected to be zero. As the numerical value of these parameters approaches zero, the properties of being a drug increase. The numerical value of all obtained parameters is given in Table 6.

The compounds have many calculated ADME parameters, but when each parameter examines a different property, it will be difficult to analyze compounds on a parameter-by-parameter basis. If we examine some important parameters; The numerical value of

the QPPCaco parameter of the compounds is generally quite high. for this reason, they have a very difficult time passing through the gut-blood barrier. The QPPMDCK parameter of the compounds is generally normal. For this reason, they can use it to be absorbed through the intestines. Percent Human Oral Absorption parameter values of compounds are at the highest level. The maximum desired for these drug compounds is 80. However, the values of the RuleOfFive and RuleOfThree parameters are zero for all compounds. It is a desired and sought value for these parameters.

**Table 6**  
ADME properties of the synthesized compounds

	4a	4b	4c	4d	4e	4f	4 g	4 h	4i	4j	4 k	4 l	4 m	Reference Range
mol_MW	319	351	359	379	305	351	341	371	342	337	307	370	319	130–725
dipole (D)	5.2	1.9	3.9	2.8	4.0	4.9	4.9	9.4	6.0	2.7	3.2	7.5	4.9	1.0–12.5
SASA	635	635	632	697	598	630	652	642	648	621	593	647	638	300–1000
FOSA	219	229	71	288	138	237	70	70	70	155	70	70	199	0–750
FISA	115	115	115	115	107	115	115	203	138	159	171	252	115	7–330
PISA	300	291	328	294	354	278	467	297	441	306	352	323	324	0–450
WPSA	0	0	118.2	0.0	0.0	0.0	0.0	72.3	0.0	0.0	0.0	1.5	0	0–175
volume (A <sup>3</sup> )	1083	1110	1073	1223	1025	1101	1118	1096	1109	1066	998	1101	1084	500–2000
donorHB	0	0	0	0	0	0	0	0	0	1	1	2	0	0–6
accptHB	4.5	6	4.5	6	4.5	6	4.5	5.5	5.5	6	5.25	9	4.5	2.0–20.0
glob (Sphere = 1)	0.8	0.8	0.8	0.8	0.8	0.8	0.8	0.8	0.8	0.8	0.8	0.8	0.8	0.75–0.95
QPpolrz (A <sup>3</sup> )	38.1	37.8	38.0	41.1	36.3	37.4	41.1	38.0	40.5	36.2	34.6	37.8	37.8	13.0–70.0
QPlogPC16	11.2	11.4	10.5	12.5	10.9	11.2	12.7	12.4	12.6	11.6	11.3	12.9	11.4	4.0–18.0
QPlogPoct	15.2	15.6	15.7	16.7	14.6	15.7	16.5	17.3	17.1	16.8	16.0	21.5	15.1	8.0–35.0
QPlogPw	7.8	8.8	8.1	8.5	8.1	8.7	9.0	9.2	10.0	10.7	10.5	15.9	7.8	4.0–45.0
QPlogPo/w	3.7	3.2	4.1	3.9	3.5	3.1	4.1	3.0	3.4	2.7	2.6	1.0	3.8	–2.0–6.5
QPlogS	–5.4	–4.3	–5.9	–5.1	–4.7	–4.2	–5.7	–5.2	–5.1	–4.6	–4.5	–4.1	–5.3	–6.5–0.5
CIQPlogS	–5.0	–5.0	–5.8	–5.5	–4.7	–5.0	–5.7	–5.6	–5.2	–4.9	–4.6	–4.4	–5.0	–6.5–0.5
QPlogHERG	–6.1	–5.9	–6.3	–6.3	–6.1	–5.8	–7.0	–6.2	–6.9	–6.0	–6.2	–6.3	–6.3	*
QPPCaco (nm/sec)	803	803	803	803	967	803	803	117	490	305	236	40	803	**
QPlogBB	–0.8	–0.9	–0.5	–1.1	–0.7	–0.9	–0.8	–1.6	–1.1	–1.3	–1.4	–2.4	–0.9	–3.0–1.2
QPPMDCK (nm/sec)	390	390	1733	390	477	390	390	121	229	137	104	16	390	**
QPlogKp	–2.3	–2.1	–2.2	–1.9	–1.9	–2.2	–1.7	–3.8	–2.2	–2.9	–3.0	–4.6	–2.1	Kp in cm/hr
IP (eV)	9.2	9.2	9.3	9.2	9.2	9.2	9.2	9.4	9.3	9.3	9.3	9.3	9.2	7.9–10.5
EA (eV)	0.6	0.6	1.0	0.6	0.6	0.6	0.7	2.6	1.0	0.6	0.6	0.9	0.6	–0.9–1.7
#metab	4	4	2	4	3	4	2	3	2	4	3	2	3	1–8
QPlogKhsa	0.4	0.0	0.4	0.3	0.3	0.0	0.5	0.2	0.2	0.1	0.1	–0.3	0.4	–1.5–1.5
Human Oral Absorption	3	3	3	3	3	3	3	3	3	3	3	3	3	–
Percent Human Oral Absorption	100	100	100	100	100	97	100	81	95	87	84	61	100	***
PSA	74	92	74	91	74	93	74	121	87	105	97	136	74	7–200
RuleOffive	0	0	0	0	0	0	0	0	0	0	0	0	0	Maximum is 4
RuleOfThree	0	0	1	0	0	0	1	0	0	0	0	0	0	Maximum is 3
Jm	0.0	0.1	0.0	0.0	0.1	0.1	0.0	0.0	0.0	0.0	0.0	0.0	0.0	–

\* concern below –5, \*\*<25 is poor and greater than 500 is great, \*\*\* <25% is poor and greater than 80% is high.

#### 4. Conclusions

In this study, 13 different benzotriazole-oxadiazole derivatives were synthesized using conventional method and ultrasonication techniques. Anticancer activity investigations of the synthesized compounds were performed against the PANC-1 cell line. Also, *in vitro* studies were also supported by computer-aided molecular docking studies. With the green chemistry technique (US) used, the reaction conditions were improved, the reaction time was shortened, the yield increased.

Currently, gemcitabine is considered the standard and only effective chemotherapeutic agent for advanced pancreatic cancer, despite showing modest results and limited survival benefit [60]. For this reason, various studies are carried out to test the cytotoxic effects of gemcitabine and other anticancer agents on PANC-1 cells to increase the therapeutic effect [61–64]. In a previous study [65], the IC<sub>50</sub> value of gemcitabine against PANC-1 cell lines was designated as 300 mM, and this value was determined to be well above the IC<sub>50</sub> value of the most effective compounds **4b** and **4d** in our study. In our further studies, we plan to examine the cytotoxic effects of compound **4d** on PANC-1 cells at wider dose ranges. In addition, the anticancer effects of compounds **4d** and **4b**, as well as cytotoxicity analyses, we also plan to evaluate Caspase 3 expressions, their effects on the cell cycle, and quantification of apoptotic proteins by western blot method. As a result of further analysis, we hope to reveal the combined treatment potential of compounds **4b** and **4d** with currently used anticancer agents in pancreatic cancer.

The theoretical studies of the compounds against pancreatic cancer proteins were compared. When the obtained docking score parameters were sorted according to the numerical value, it was seen that compound **4d** had the highest activity with –8.71 kcal/mol versus docking score parameter (ID: 6HP9) and docking score

parameter with –9.52 kcal/mol (ID: 5E80). After examining the interactions of molecules and proteins, ADME calculations were made to examine the drug properties of molecules. It has been seen that the numerical value of the parameters obtained from these calculations is in the desired range. These calculations will be an important guide for future in-vivo experiments.

#### CRediT authorship contribution statement

**Arif Mermer:** Conceptualization, Methodology, Writing – original draft, Visualization, Supervision, Writing – review & editing. **Muhammet Volkan Bulbul:** Investigation, Methodology, Writing – original draft. **Semiha Mervener Kalender:** Investigation, Methodology. **Ilknur Keskin:** Investigation, Methodology, Writing – original draft. **Burak Tuzun:** Methodology, Formal analysis, Writing – original draft. **Ozan Emre Eyupoglu:** Methodology, Formal analysis, Writing – original draft.

#### Declaration of Competing Interest

The authors declare that they have no known competing financial interests or personal relationships that could have appeared to influence the work reported in this paper.

#### Acknowledgements

This work was supported by Scientific Research Project Fund of University of Health Sciences-Turkey (Project no: 2019/097) This work is supported by the Scientific Research Project Fund of Sivas Cumhuriyet University under the project number RGD-020. This research was made possible by TUBITAK ULAKBIM, High Performance and Grid Computing Center (TR-Grid e-Infrastructure).



## References

- [1] H. Rashid, Y. Xu, Y. Muhammad, L. Wang, J. Jiang, Research advances on anticancer activities of matrine and its derivatives: an updated overview, *Eur. J. Med. Chem.* 161 (2019) 205–238, <https://doi.org/10.1016/j.ejmech.2018.10.037>.
- [2] F. Gao, X. Zhang, T.F. Wang, J.Q. Xiao, Quinolone hybrids and their anti-cancer activities: an overview, *Eur. J. Med. Chem.* 165 (2019) 59–79, <https://doi.org/10.1016/j.ejmech.2019.01.017>.
- [3] World Health Organization, **Latest global cancer data: cancer burden rises to 18.1 million new cases and 9.6 million cancer deaths in 2018**, International Agency for Research on Cancer, 263 (2018), pp. 1–3.
- [4] World Health Organization, **Cancer: key facts**, <http://www.who.int/newsroom/fact-sheets/detail/cancer>, Accessed Date: 11.12.2020.
- [5] World Health Organization, **Cancer control: knowledge into action**, <http://www.who.int/cancer/modules/en/>, Accessed Date: 11.12.2020.
- [6] M. Ilic, I. Ilic, Epidemiology of pancreatic cancer, *World J Gastroenterol* 22 (2016) 9694–9705, <https://doi.org/10.3748/wjg.v22.i44.9694>.
- [7] R. Siegel, K. Miller, A. Jemal, Cancer statistics, *CA Cancer J Clin* 65 (2015) (2015) 5–29, <https://doi.org/10.3322/caac.21254>.
- [8] C.C. Reyes-Gibby, W. Chan, J.L. Abbruzzese, H.Q. Xiong, L. Ho, D.B. Evans, et al., Patterns of self-reported symptoms in pancreatic cancer patients receiving chemoradiation, *J Pain Symptom Manage* 34 (2007) 244–252, <https://doi.org/10.1016/j.jpainsymman.2006.11.007>.
- [9] M. Löhr, Is it possible to survive pancreatic cancer?, *Nat Clin Pract Gastroenterol Hepatol* 3 (2006) 236–237, <https://doi.org/10.1038/npcgasthep0469>.
- [10] A. Vincent, J. Herman, R. Schulick, R.H. Hruban, M. Goggins, Pancreatic cancer, *The Lancet* 378 (2011) 607–620, [https://doi.org/10.1016/S0140-6736\(10\)62307-0](https://doi.org/10.1016/S0140-6736(10)62307-0).
- [11] M.S. Islam, C.Y. Wang, J.Y. Zheng, N. Paudyal, Y.L. Zhu, H.X. Sun, The potential role tubeimosides in cancer prevention and treatment, *Eur. J. Med. Chem.* 162 (2019) 109–121, <https://doi.org/10.1016/j.ejmech.2018.11.001>.
- [12] Z.X. Qing, J.L. Huang, X.Y. Yang, J.H. Liu, H.L. Cao, F. Xiang, P. Cheng, J.G. Zeng, Anticancer and reversing multidrug resistance activities of natural isoquinoline alkaloids and their structure–activity relationship, *Curr. Med. Chem.* 25 (2018) 5088–5114, <https://doi.org/10.2174/0929867324666170920125135>.
- [13] L. Wang, C. Dong, X. Li, W. Han, X. Su, Anticancer potential of bioactive peptides from animal sources, *Oncol. Rep.* 38 (2017) 637–651, <https://doi.org/10.3892/or.2017.5778>.
- [14] N.D. Gaikwad, S.V. Patil, V.D. Bobade, Synthesis and biological evaluation of some novel thiazole substituted benzotriazole derivatives, *Bioorg Med Chem Lett.* 22 (2012) 3449–3454, <https://doi.org/10.1016/j.bmcl.2012.03.094>.
- [15] (a) J. Das, C.V.L. Rao, T.V.R.S. Sastry, et al., **Effects of positional and geometrical isomerism on the biological activity of some novel oxazolidinones**, *Bioorg Med Chem Lett.* 2005(2005), pp. 337–343; (b) Z. Rezaei, S. Khabnadideh, K. Zomorodian, et al., **Design, synthesis and antifungal activity of some new imidazole and triazole derivatives**, *Arch Pharm Chem Life Sci.* 344 (2011), pp. 658–665; (c) M. Bretner, A. Baier, K. Kopanska, et al., **Synthesis and biological activity of 1Hbenzotriazole and 1H-benzimidazole analogues–inhibitors of the NTPase/helicase of HCV and of some related Flaviviridae**, *Antiviral Chem Chemother.* 16 (2005), pp. 315–326; (d) A. Rajasekaran, K.A. Rajagopal, **Synthesis of some novel triazole derivatives as anti-nociceptive and anti-inflammatory agents**, *Acta Pharm.* 59 (2009), pp. 355–364; (e) G. Caliendo, R.D. Carlo, R. Meli, et al., **Synthesis and trazodone-like pharmacological profile of 1- and 2-[3-[4-(X)-1-piperazinyl]-propyl]-benzotriazoles**, *Eur J Med Chem.* 28 (1993), pp. 969–1674; (f) I. Briguglio, S. Piras, P. Corona, E. Gavini, M. Nieddu, B.A. Carta, **Benztiazole: An overview on its versatile biological behavior**, *Eur J Med Chem.* 97 (2015), pp. 612–648.
- [16] R.R. Somani, P.Y. Shirodkar, Oxadiazole: a biologically important heterocycle, *Der Pharma Chem.* 1 (2009) 130–140, <https://doi.org/10.1002/chin.201110251>.
- [17] A.A. Ziyayev, D.S. Ismailova, **Biological activity of 5-(2,3,4-pyridyl)-1,3,4-oxadiazol-2- thiones and their derivatives**, *World J Pharm Res.* 6 (2017) 52–77, <https://doi.org/10.20959/wjpr20174-8107>.
- [18] R. Sharma, N. Kumar, R. Yadav, **Chemistry and pharmacological importance of 1,3,4-oxadiazole derivatives**, *Res Rev J Chem.* 4 (2015) 1–27.
- [19] A. Mermer, O. Faiz, A. Demirbas, N. Demirbas, M. Alagumuthu, S. Arumugam, Piperazine-azole-fluoroquinolone hybrids: conventional and microwave irradiated synthesis, biological activity screening and molecular docking studies, *Bioorg. Chem.* 85 (2019) 308–318, <https://doi.org/10.1016/j.bioorg.2019.01.009>.
- [20] S.S. Dea, M.P. Khambete, M.S. Degani, Oxadiazole scaffolds in anti-tuberculosis drug discovery, *Bioorg Med Chem Lett.* 29 (2019) 1999–2007, <https://doi.org/10.1016/j.bmcl.2019.06.054>.
- [21] A.R. Gulnaz, Y.H.E. Mohammed, S.A. Khanum, **Design, synthesis and molecular docking of benzophenone conjugated with oxadiazole sulphur bridge pyrazole pharmacophores as anti inflammatory and analgesic agents**, *Bioorganic Chemistry* 92 (2019).
- [22] F.A.V. Rodrigues-Vendramini, D.R. Faria, G.S. Arita, I.R.G. Capoci, K.M. Sakita, S. M. Caparroz-Assef, et al., Antifungal activity of two oxadiazole compounds for the paracoccidiodomycosis treatment, *PLoS Negl Trop Dis* 13 (2019), <https://doi.org/10.1371/journal.pntd.0007441> e0007441.
- [23] M.D. Altıntop, B. Sever, G. Akalın Çiftçi, G. Turan-Zitouni, Z.A. Kaplancıklı, A. Ozdemir, Design, synthesis, in vitro and in silico evaluation of a new series of oxadiazole-based anticancer agents as potential Akt and FAK inhibitors, *Eur J Med Chem.* 155 (2018) 905–924, <https://doi.org/10.1016/j.ejmech.2018.06.049>.
- [24] B. Meunier, Hybrid molecules with a dual mode of action: dream or reality?, *Acc Chem. Res.* 41 (2008) 69–77, <https://doi.org/10.1021/ar7000843>.
- [25] S.S. Mishra, P. Singh, Hybrids molecules: the privileged scaffolds for various pharmaceuticals, *Eur. J. Med. Chem.* 124 (2016) 500–536, <https://doi.org/10.1016/j.ejmech.2016.08.039>.
- [26] Z. Xu, S.J. Zhao, Z.S. Lv, F. Gao, J.L. Deng, Fluoroquinolone-isatin hybrids and their biological activities, *Eur. J. Med. Chem.* 162 (2019) 396–406, <https://doi.org/10.1016/j.ejmech.2018.11.032>.
- [27] N. Kerru, P. Singh, N. Koorbanally, R. Raj, V. Kumar, Recent advances (2015–2016) in anticancer hybrids, *Eur. J. Med. Chem.* 142 (2017) 179–212, <https://doi.org/10.1016/j.ejmech.2017.07.033>.
- [28] S. Akkoç, B. Tüzün, A. Özalp, Z. Kökbudak, Investigation of structural, electrical and in vitro cytotoxic activity properties of some heterocyclic compounds, *J. Mol. Struct.* 1246 (2021) 131127.
- [29] A.N. Khailov, B. Tüzün, P. Taslimi, A. Tas, Z. Tuncbilek, Cytotoxic effect, spectroscopy, DFT, enzyme inhibition, and molecular docking studies of some novel mesitylaminopropanols: antidiabetic and anticholinergics and anticancer potentials, *J. Mol. Liq.* 117761 (2021).
- [30] D. Zhu, H. Huang, D.M. Pinkas, J. Luo, D. Ganguly, A.E. Fox, X. Lu, 2-Amino-2, 3-dihydro-1 H-indene-5-carboxamide-based discoidin domain receptor 1 (DDR1) inhibitors: design, synthesis, and in vivo antipneumonia cancer efficacy, *J. Med. Chem.* 62 (2019) 7431–7444, <https://doi.org/10.1021/acs.jmedchem.9b00365>.
- [31] B. Papke, S. Murarka, H.A. Vogel, P. Martín-Gago, M. Kovacevic, D.C. Truxius, P.I. Bastiaens, Identification of pyrazolopyridazinones as PDE5 inhibitors, *Nat. Commun.* 7 (2016) 11360, <https://doi.org/10.1038/ncomms11360>.
- [32] N.I. Taha, Synthesis of 1,3-Oxazepine Derivatives Derived from 2-(1H-Benzo[d][1,2,3] Triazol-1-yl) Acetohydrazide by Using Microwave Irradiation, *J. Org. Chem.* 7 (2017) 219–228, <https://doi.org/10.4236/joc.2017.73016>.
- [33] Y. Luo, L. Zhi-Jun, G. Chen, L. Jing-Ran, S. Jing, Z. Hai-Liang, 1,3,4-Oxadiazole derivatives as potential antitumor agents: discovery, optimization and biological activity evaluation, *Med. Chem. Commun.* 7 (2015) 263–271, <https://doi.org/10.1039/C5MD00371G>.
- [34] Schrödinger Release 2021-3: **Maestro**, Schrödinger, LLC, New York, NY, 2021.
- [35] Schrödinger Release 2019-4: **Protein Preparation Wizard**; **Epik**, Schrödinger, LLC, New York, NY, 2016; **Impact**, Schrödinger, LLC, New York, NY, 2016; **Prime**, Schrödinger, LLC, New York, NY, 2019.
- [36] Schrödinger Release 2021-3: **LigPrep**, Schrödinger, LLC, New York, NY, 2021.
- [37] M. Erdogan, P. Taslimi, B. Tuzun, Synthesis and docking calculations of tetrafluoronaphthalene derivatives and their inhibition profiles against some metabolic enzymes, *Archiv der Pharmazie* 354 (2021), <https://doi.org/10.1002/ardp.202000409> e2000409.
- [38] Schrödinger Release 2021-3: **QikProp**, Schrödinger, LLC, New York, NY, 2021.
- [39] M.V. Bulbul, S. Karabulut, M. Kalender, I. Keskin, Effects of gallic acid on endometrial cancer cells in two and three dimensional cell culture models, *Asian Pacific Journal of Cancer Prevention: APJCP* 22 (6) (2021) 1745.
- [40] R.B. Singh, G.K. Singh, K. Chaturvedi, D. Kumar, S.K. Singh, K. Zaman, Design, synthesis, characterization, and molecular modeling studies of novel oxadiazole derivatives of nipecotic acid as potential anticonvulsant and antidepressant agents, *Med Chem Res* 27 (2018) 137–152, <https://doi.org/10.1007/s00044-017-2047-y>.
- [41] A. Mermer, N. Demirbas, A. Demirbas, N. Colak, F.A. Ayaz, M. Alagumuthu, S. Arumugam, Synthesis, biological activity and structure activity relationship studies of novel conazole analogues via conventional, microwave and ultrasound mediated techniques, *Bioorg. Chem.* 81 (2018) 55–70, <https://doi.org/10.1016/j.bioorg.2018.07.036>.
- [42] A. Mermer, N. Demirbas, U. Cakmak, A. Colak, A. Demirbas, M. Alagumuthu, S. Arumugam, **Discovery of Novel Sulfonamide-Based 5-Arylidenerhodanines as Effective Carbonic Anhydrase (II) Inhibitors: Microwave-Assisted and Ultrasound-Assisted One-Pot Four-Component Synthesis, Molecular Docking, and Anti-CA II Screening Studies**, *J. Het Chem.* 56 (2019) 2460–2468, <https://doi.org/10.1002/jhet.3635>.
- [43] A. Mermer, N. Demirbas, H. Uslu, A. Demirbas, S. Ceylan, Y. Sirin, Synthesis of novel Schiff bases using green chemistry techniques; antimicrobial, antioxidant, antiurease activity screening and molecular docking studies, *J. Mol. Struct.* 1181 (2019) 412–422, <https://doi.org/10.1016/j.molstruc.2018.12.114>.
- [44] Z. Yaping, B. Shurui, Curcumin induces autophagy, apoptosis, and cell cycle arrest in human pancreatic cancer cells, *eCAM* (2017 (2017),) 1–13, <https://doi.org/10.1155/2017/5787218>.
- [45] A. Moayedi, J. Nowroozi, A.A. Sepahy, Cytotoxic effect of pyocyanin on human pancreatic cancer cell line (Panc-1), *Iranian Journal of Basic Medical Sciences* 21 (8) (2018) 794.
- [46] M.A. Marsooli, M. Fasihi-Ramandi, K. Adib, S. Pourmasoud, F. Ahmadi, M.R. Ganjali, A. Sobhani Nasab, M.R. Nasrabadi, M.E. Plonska-Brzezinska, Preparation and characterization of magnetic Fe<sub>3</sub>O<sub>4</sub>/CdWO<sub>4</sub> and Fe<sub>3</sub>O<sub>4</sub>/CdWO<sub>4</sub>/PrVO<sub>4</sub> nanoparticles and investigation of their photocatalytic and anticancer properties on PANC1 cells, *Materials (Basel)* 12 (2019) 3274, <https://doi.org/10.3390/ma12193274>.
- [47] R. Tang, Z. Dongyi, K. Atsushi, S. Andi, A. Masayoshi, Selective cytotoxicity of marine-derived fungal metabolite (3 S, 6 S)-3, 6-dibenzylpiperazine-2, 5-dione

- against cancer cells adapted to nutrient starvation, *J. Antibiot.* 73 (2020) 873–875, <https://doi.org/10.1038/s41429-020-0340-3>.
- [48] C. Ding, M. Khan, B. Zheng, J. Yang, L. Zhong, T. Ma, Casticin induces apoptosis and mitotic arrest in pancreatic carcinoma PANC-1 cells, *Afr. J. Pharmacy Pharmacol.* 6 (2012) 412–418, <https://doi.org/10.5897/AJPP11.830>.
- [49] K.S. Crump, D.G. Hoel, C.H. Langley, R. Peto, Fundamental carcinogenic processes and their implications for low dose risk assessment, *Cancer Res.* 36 (1976) 2973–2979.
- [50] H. Poppenga Robert, S. Wayne, **Veterinary toxicology**, *Information Resources in Toxicology*, Academic Press (2009) 515–522.
- [51] S.C. Yavuz, S. Akkoc, B. Tuzun, O. Sahin, E. Saripinar, Efficient synthesis and molecular docking studies of new pyrimidine-chromeno hybrid derivatives as potential antiproliferative agents, *Synth. Commun.* 51 (2021) 2135–2159, <https://doi.org/10.1080/00397911.2021.1922920>.
- [52] P. Taslimi, F. Akhundova, M. Kurbanova, F. Turkan, B. Tuzun, A. Sujayev, N. Sadeghian, A. Maharramov, V. Farzaliyev, I. Gulcin, Biological activity and molecular docking study of some bicyclic structures: antidiabetic and anticholinergic potentials, *Polycycl. Aromat. Compd.* (2021) 1–14, <https://doi.org/10.1080/10406638.2021.1981405>.
- [53] P. Taslimi, Y. Demir, H.E. Duran, U.M. Kocyigit, B. Tuzun, O.N. Aslan, M. Ceylan, & I. Gulcin, **Some old 2-(4-(Aryl)-thiazole-2-yl)-3a, 4, 7, 7a-tetrahydro-1H-4, 7-tethanoisindole-1, 3 (2H)-dione derivatives: Synthesis, inhibition effects and molecular docking studies on aldose reductase and  $\alpha$ -glycosidase**, *CSJ*, 42 (2021), pp. 553–564, 10.17776/csj.897800.
- [54] A.T. Bilgili, T. Kandemir, B. Tuzun, R. Ariduru, A. Günsel, C. Abak, M.N. Yarasir, G. Arabaci, Octa-substituted Zinc (II), Cu (II), and Co (II) phthalocyanines with 1-(4-hydroxyphenyl) propane-1-one: Synthesis, sensitive protonation behaviors, Ag (I) induced H-type aggregation properties, antibacterial-antioxidant activity, and molecular docking studies, *Appl. Organomet. Chem.* 35 (2021), <https://doi.org/10.1002/aoc.6353> e6353.
- [55] D. Majumdar, B. Tuzun, T.K. Pal, R.V. Saini, K. Bankura, D. Mishra, Structurally diverse heterobimetallic Pb (II)-Salen complexes mechanistic notion of cytotoxic activity against neuroblastoma cancer cell: Synthesis, characterization, protein-ligand interaction profiler, and intuitions from DFT, *Polyhedron* 210 (2021), <https://doi.org/10.1016/j.poly.2021.115504> 115504.
- [56] M.B. Gurdere, Y. Budak, U.M. Kocyigit, P. Taslimi, B. Tuzun, M. Ceylan, ADME properties, bioactivity and molecular docking studies of 4-amino-chalcone derivatives: new analogues for the treatment of Alzheimer, glaucoma and epileptic diseases, *In Silico Pharmacol.* 9 (2021) 34, <https://doi.org/10.1007/s40203-021-00094-x>.
- [57] C.A. Lipinski, Lead-and drug-like compounds: the rule-of-five revolution, *Drug Discov. Today: Technol.* 1 (2004) 337–341, <https://doi.org/10.1016/j.ddtec.2004.11.007>.
- [58] C.A. Lipinski, F. Lombardo, B.W. Dominy, P.J. Feeney, Experimental and computational approaches to estimate solubility and permeability in drug discovery and development settings, *Adv. Drug Deliv. Rev.* 46 (2001) 3–26, [https://doi.org/10.1016/s0169-409x\(00\)00129-0](https://doi.org/10.1016/s0169-409x(00)00129-0).
- [59] W.J. Jorgensen, E.M. Duffy, Prediction of drug solubility from structure, *Adv. Drug Deliv. Rev.* 54 (2002) 355–366, [https://doi.org/10.1016/s0169-409x\(02\)00008-x](https://doi.org/10.1016/s0169-409x(02)00008-x).
- [60] N.P. Pereira, J.R. Corrêa, Pancreatic cancer: treatment approaches and trends, *J. Cancer Metastasis Treat* 4 (2018) 30, <https://doi.org/10.20517/2394-4722.2018.13>.
- [61] L. Dong, J. Yun-Ming, C. Pi-Kun, W. Wei, L. Bin, L. Yu-Liang, Combined effect of 125I and gemcitabine on PANC-1 cells: cellular apoptosis and cell cycle arrest, *J. Cancer Res Ther* 14 (2018) 1476–1481, [https://doi.org/10.4103/jcrt.jcrt\\_43\\_18](https://doi.org/10.4103/jcrt.jcrt_43_18).
- [62] S. Jiang, D.L. Li, J. Chen, X. Zheng, P.P. Wu, C. Li, X.T. Xu, K. Zhang, Synergistic anticancer effect of gemcitabine combined with impressic acid or acankoreanogin in Panc-1 cells by inhibiting NF- $\kappa$ B and Stat 3 activation 1934578X20974239 *Natural Product Communications* 15 (12) (2020), <https://doi.org/10.1177/1934578X20974239>.
- [63] C. Serri, V. Quagliariello, R.V. Iaffaioli, S. Fusco, G. Botti, L. Mayol, M. Biondi, Combination therapy for the treatment of pancreatic cancer through hyaluronic acid-decorated nanoparticles loaded with quercetin and gemcitabine: A preliminary in vitro study, *J. Cell. Physiol.* 234 (2019) 4959–4969, <https://doi.org/10.1002/jcp.27297>.
- [64] H.A. El-Mahdy, A.A. El-Husseiny, Y.I. Kandil, A.M.G. El-Din, Diltiazem potentiates the cytotoxicity of gemcitabine and 5-fluorouracil in PANC-1 human pancreatic cancer cells through inhibition of P-glycoprotein, *Life Sci.* 262 (2020), <https://doi.org/10.1016/j.lfs.2020.118518>.
- [65] R.A. Fryer, B. Barlett, C. Galustian, A.G. Dalgleish, Mechanisms underlying gemcitabine resistance in pancreatic cancer and sensitisation by the iMid<sup>TM</sup> lenalidomide, *Anticancer Res.* 31 (2011) 3747–3756.